# Intravital microscopy for real-time monitoring of drug delivery and nanobiological processes

Advanced Drug Delivery Reviews 189 (2022) 114528

Contents lists available at ScienceDirect

Advanced Drug Delivery Reviews

journal homepage: www.elsevier.com/locate/adr

# Intravital microscopy for real-time monitoring of drug delivery and nanobiological processes

Jeffrey Momoh [a], Dimitrios Kapsokalyvas [b,c], Michael Vogt [c], Sjoerd Hak [d,e], Fabian Kiessling [a], Marc van Zandvoort [f,g,*], Twan Lammers [a,*], Alexandros Marios Sofias [a,e,h,*]

[a] Department of Nanomedicine and Theranostics, Institute for Experimental Molecular Imaging, Faculty of Medicine, RWTH Aachen University, Aachen, Germany
[b] Department of Genetics and Cell Biology, Maastricht University, Maastricht, the Netherlands
[c] Interdisciplinary Center for Clinical Research (IZKF), University Hospital RWTH Aachen University, Aachen, Germany
[d] Department of Biotechnology and Nanomedicine, SINTEF Industry, Trondheim, Norway
[e] Department of Circulation and Medical Imaging, Faculty of Medicine and Health Sciences, Norwegian University of Science and Technology (NTNU), Trondheim, Norway
[f] Department of Genetics and Cell Biology, School for Cardiovascular Diseases CARIM, School for Oncology and Reproduction GROW, School for Mental Health and Neuroscience MHeNS, Maastricht University, Maastricht, the Netherlands
[g] Institute for Molecular Cardiovascular Research (IMCAR), University Hospital RWTH Aachen University, Aachen, Germany
[h] Mildred Scheel School of Oncology (MSSO), Center for Integrated Oncology Aachen Bonn Cologne Duesseldorf (CIO$^{ABCD}$), University Hospital Aachen, Aachen, Germany

ARTICLE INFO

*Article history:*
Received 22 April 2022
Revised 10 August 2022
Accepted 30 August 2022
Available online 5 September 2022

*Keywords:*
Intravital microscopy
Confocal microscopy
Multiphoton microscopy
Nanomedicine
Drug delivery
Immunotherapy
Pharmacokinetics
Biodistribution
Drug targeting
Tumor microenvironment

ABSTRACT

Intravital microscopy (IVM) expands our understanding of cellular and molecular processes, with applications ranging from fundamental biology to (patho)physiology and immunology, as well as from drug delivery to drug processing and drug efficacy testing. In this review, we highlight modalities, methods and model organisms that make up today's IVM landscape, and we present how IVM - via its high spatiotemporal resolution - enables analysis of metabolites, small molecules, nanoparticles, immune cells, and the (tumor) tissue microenvironment. We furthermore present examples of how IVM facilitates the elucidation of nanomedicine kinetics and targeting mechanisms, as well as of biological processes such as immune cell death, host-pathogen interactions, metabolic states, and disease progression. We conclude by discussing the prospects of IVM clinical translation and examining the integration of machine learning in future IVM practice.



**Contents**



* Corresponding authors at: Department of Genetics and Cell Biology, School for Cardiovascular Diseases CARIM, School for Oncology and Reproduction GROW, School for Mental Health and Neuroscience MHeNS, Maastricht University, Maastricht, the Netherlands (M. van Zandvoort). Department of Nanomedicine and Theranostics, Institute for Experimental Molecular Imaging, Faculty of Medicine, RWTH Aachen University, Aachen, Germany (T. Lammers, A.M. Sofias).
*E-mail addresses:* mamj.vanzandvoort@maastrichtuniversity.nl (M. van Zandvoort), tlammers@ukaachen.de (T. Lammers), asofias@ukaachen.de (A.M. Sofias).

https://doi.org/10.1016/j.addr.2022.114528
0169-409X/

## 1. Introduction

In the last three decades, advances in microscopy technology have boosted the integration of IVM in preclinical research. In parallel, the production of high spatiotemporal resolution data enabling the real-time *in vivo* monitoring of (nano-) drug behavior and biological processes has considerably improved. Initially, IVM was based on brightfield imaging that was allowing the imaging of (semi-) transparent systems. As such, the earliest applications focused on the characterization of blood flow and immune cell recruitment in easily accessible regions, such as the vasculature of the open cremaster muscle.

Exploration of tissues with higher structural complexity and less accessibility arose later, with the advent of fluorescence microscopy and the development of fluorescent probes. In this regard, confocal and multiphoton microscopy (MPM) initially dominated the IVM landscape, allowing for visualization of multiple fluorophores at a considerable penetration depth. In addition, the ability of IVM to function at sub-second temporal and sub-micrometer spatial resolution has provided researchers with the tools to record dynamic biological processes *in vivo*. Considering the clear trend in the medical imaging field to go towards multiscale and multimodal imaging, IVM complements traditional non-invasive imaging modalities, such as MRI, PET, FMT and CT, which allow for real-time whole-body imaging at a much larger (millimeter) scale [1–7].

IVM has reinforced our ability to answer scientific questions that seemed inaccessible a decade ago. Such challenges e.g., include the visualization of drug distribution at the tissue level, of swift metabolic responses upon applying certain stimuli, of individual immune cells' behavior, as well as of alterations in tumor microenvironment (TME) composition during disease progression or (targeted) therapy. IVM has contributed prominently to the field of nanomedicine, by deciphering the various passive and active targeting mechanisms that drug delivery systems employ to interact with host organs and cells, as well as with target tissues. A broad timeline of technologies and achievements in intravital microscopy is presented in Fig. 1 [8–30]. In this manuscript, we provide an overview of contemporary IVM technology and applications, exemplifying its value for investigating complex drug delivery and biological processes *in vivo* at very high spatiotemporal resolution.

## 2. Intravital microscopy: technical aspects and model organisms

### 2.1. Technical aspects

In intravital microscopy (IVM), the biological process to be investigated very much determines the methodology used. Factors such as penetration depth, spatial resolution, recording speed, and sensitivity are important selection criteria. In addition, accessibility and preparation of the area of interest play a crucial role in IVM based on brightfield microscopy. Indeed, it is limited to transparent and thin tissues (5–10 μm), which restricts the application to for example mouse mesenteric tissue and cremaster muscle. It requires special sample preparation, e.g., externalizing and flattening of the tissue. Advanced IVM is typically based on the principle of fluorescence emission of the sample. Fluorescence microscopy enables selective staining, however, is still limited to relatively thin specimens (5–10 μm). In thicker samples, scattered light interferes with the detection of the primary signal and results in blurry images.

This problem is solved by the more advanced fluorescence microscopy methods, such as confocal or multiphoton laser scanning microscopy. These expand the list of possible applications by achieving greater penetration depths, while simultaneously reaching significantly improved subcellular resolutions. The exact value of tissue penetration depends on the technique used, tissue optical properties, and preparation of the animal.

In confocal laser scanning microscopy (CLSM), laser light is focused on the sample to sequentially point-scan a region of interest. Axial sectioning of the sample is achieved by using a pinhole, which rejects out-of-focus light, and axially translating the objective, thus focusing at different depths inside the sample. This improves resolution (~200 nm) and contrast but at the cost of speed since each point is individually imaged [31,32]. It is important to note that the advantage of confocal microscopy is lost at higher depth (over 50 μm), due to scattering of both the excitation and emission light. Therefore, only IVM applications with a relatively low penetration depth are feasible.

Multiphoton laser scanning microscopy (MPLSM) is based on the absorption of two or more photons by a fluorescent marker. In Two-photon microscopy (2PLSM), two photons of half the energy than normally needed (i.e., double the wavelength)

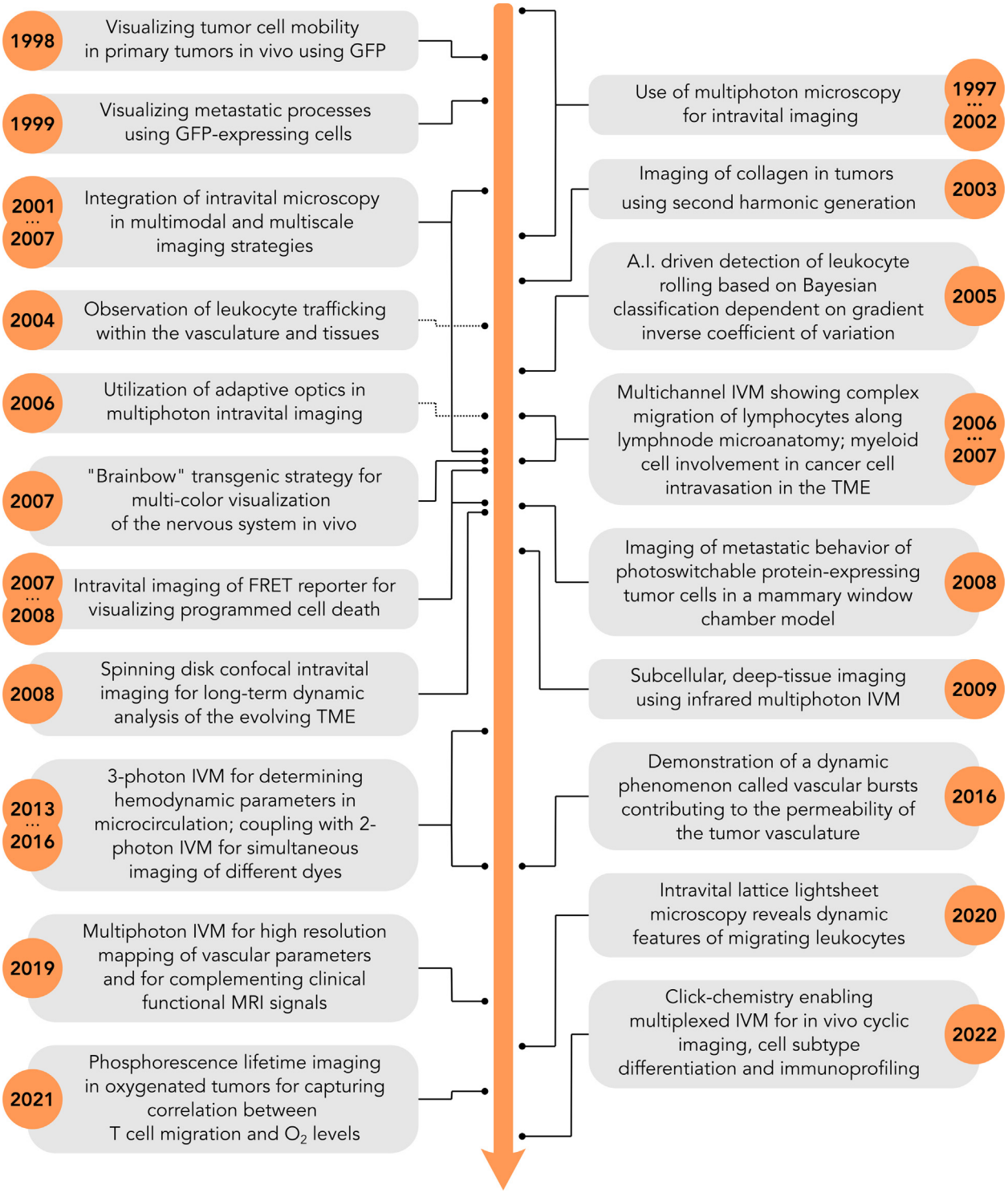


**Fig. 1.** A timeline of key advances and technologies beginning from one of the earliest uses of GFP in intravital microscopy of primary and metastatic tumors. The listed events are characterized by the use of new technologies that have enabled the discovery of novel processes and (patho)physiological events.

together excite the molecule, followed by deexcitation through the emission of fluorescence [33]. Due to the nominal probability of 2 photon absorption, the excitation can only occur in the narrow focus of a pulsed near-infrared laser with short pulse duration (100 fs) and high repetition rate (80 MHz). This omits the need of a pinhole, allowing detectors to be placed closer to the sample. In addition, near-infrared light penetrates deeper into scattering tissues, allowing excitation deeper inside the sample. As a result, 2PLSM has an improved penetration depth with excellent resolution in three dimensions, even at larger depths [34]. This makes 2PLSM preferable over other fluorescence microscopic techniques, for visualizing structures in three dimensions regarding IVM.

New broad range lasers open up the utilization of far-red dyes, which allow for even deeper penetration, due to less light scattering within the sample. Furthermore, at longer excitation wavelengths, the possibility of three-photon excitation becomes viable

[35,36]. Comparable to two-photon excitation, in three-photon excitation, the fluorophore simultaneously absorbs three photons of one third the energy normally needed (i.e., three times that wavelength). In 3PLSM, the fluorescence that follows is thus even more localized than in 2PLSM. Intravital 3PLSM has mostly been used in neuroscience to visualize vascular and neuronal structures [11,37].

With the use of pulsed lasers in MPLSM, fluorescence lifetime imaging microscopy (FLIM) is emerging as another promising contrast method [38]. FLIM uses the unique fluorescence lifetime of fluorescent dyes for imaging and represents a decisive advance in microscopy, enabling the representation of different dyes, even with spectral overlap, or physiological changes of the fluorescence reporters. In FLIM, image contrast is created using the fluorescence lifetime of a fluorophore instead of (and entirely independent from) fluorescence intensity. The fluorescence lifetime of a fluorophore changes, with differences in its (bio-) chemical environment (e.g., changes in pH, viscosity and interactions with proteins). After a pulsed laser excitation, the exponential decline in fluorescence of counted photons per pixel is measured. So far, its translation into IVM has proven challenging, owing to the extensive offline analysis needed and the associated slow imaging speed. Though, with the implementation of fast FLIM imaging, the adaptation into IVM has come in reach [38]. FLIM has already been extensively used in autofluorescent molecular imaging, where it can be used to study cellular metabolism. FLIM therefore increases the image information in a single IVM experiment, which is relevant in view of the complexity of experimental set-up of IVM experiments and the need of animals.

In recent years, light sheet microscopy (LSM) has come to be the leading IVM technique for imaging developmental biology and pathology in embryos, *C. Elegans*, zebrafish, and Drosophila. In light sheet microscopy, the sample is illuminated with a thin sheet of light that serves as single-photon excitation source for the fluorescent probe. In this sheet, fluorescence emission takes place, while no fluorescence excitation occurs outside of the sheet. The fluorescence is then detected with an objective perpendicular to the excitation source [39,40]. Specific advantages of light sheet microscopy are the low light doses needed (thus limiting photodamage), its intrinsic speed, and its rather simple widefield geometry. However, it is only applicable in transparent samples due to its need for the light sheet to penetrate and its detection under 90 degrees. Furthermore, sample inclusion often is difficult. Recently the implementation of lattice light sheet microscopy a super-resolution variant of LSM has also been demonstrated. Big volume IVM imaging of dynamic process has been demonstrated with resolution in the order of 300 nm [41].

The advent of super-resolution microscopy, i.e., techniques that overcome the traditional diffraction-limited resolution of roughly half the wavelength used, has opened further possibilities for IVM, by increasing the resolution to the nanometer range. While lateral resolutions in diffraction limited techniques as discussed so far are between 250 and 400 nm range, techniques such as PALM/STORM can provide a resolution of around 20 nm, however they are based on widefield configuration with limited depth capabilities, therefore limiting their applicability for IVM. Structured illumination microscopy (SIM) on the other hand only offers a 2-fold lateral resolution improvement (~120 nm) over classical widefield microscopy, however when combined with scanning techniques it can have sectioning capabilities and therefore provide 3D imaging [42]. Its attractiveness is based on the possibility to use standard fluorescent probes. Stimulated emission depletion (STED), based on the confocal principle, employs additionally a depletion laser to shrink the effective point spread function (PSF), narrowing down its dimension to 50 nm. As in confocal microscopy, for IVM its penetration depth often is the limit, but that can further be enhanced by combining it with two-photon excitation. STED has been employed for IVM, particularly for brain imaging [43]. However, the problem of STED is often the high light doses needed and the availability of, at least currently, a limited set of fluorescent markers, since these require special properties.

Fairly new is the use of confocal and multiphoton endoscopy to image intravitally in locations not accessible via an external path, such as bladder, placenta. This field started with the development of small confocal endoscopes (with all the (dis)advantages described above), followed by a move towards the field of multiphoton endoscopy, specifically via the development of small brain-attachable microscopes for imaging brain activity while mice are active. Multiphoton endoscopic IVM promises to combine all the advantages of multiphoton bulk microscopy with easy access to locations inside the animal. However, the realization of proper guidance of the excitation source through a fiber to arrive at truly flexible endoscopes has appeared to be a tough issue. The implementation of optical fibers has enabled true flexibility in general endoscopic imaging. However, due to the fundamental nature of nonlinear optics, implementation of this technology in such imaging systems remains challenging.

All the various microscopic modalities used for intravital imaging ultimately aim to monitor and elucidate dynamics of cells and dynamic biological processes in multiple organs that cannot possibly be gained using ex vivo methods. In this regard, IVM is a stepping stone towards in-patient imaging. The development of these techniques depends on suppression of experimental motional artifacts. Even anesthetized animals show motions (breathing, heart beat), which may result in decreased spatial and temporal resolution, and can limit acquisition time. Furthermore, tissue-preparation artifacts like shrinkage, dehydration, and tearing are relevant processes to consider, as such artifacts will significantly alter the histological landscape and will therefore distort discernibility of depicted features. The same accounts for imaging-induced artifacts, such as photobleaching, autofluorescence, low signal to noise ratio, and light absorbance by blood. Photobleaching, especially, can significantly limit the choice of fluorophore and modality, as well as restrict the range of exposure/acquisition time and imaging depth. Indeed, the usefulness of IVM depends on not interfering with normal biological processes. These issues can only be addressed by acknowledging and trying to minimize them, e.g., by adaptations in the experimental setup, such as anesthesia by mechanical ventilation, image triggering for reducing motion artifacts, and use of resonant scanning microscopy. Where necessary also post-acquisition image processing can be used for correction and is a prerequisite for reliable data evaluation [44]. There exist a number of examples in literature discussing suitable protocols, methodologies and equipment for intravital microscopy [45–47].

### 2.2. Model organisms

There are several key model organisms routinely employed in IVM. The most common ones are small and transparent organisms, such as *C. elegans* and zebrafish embryos, although, small rodents such as mice and rats also find frequent application, especially in biomedical research [2]. IVM has been applied to larger animals such as rabbits or macaques for imaging external organs such as the eye [48,49]. Similar applications have also even been considered possible in humans *in vivo* [50]. For preclinical research, the choice of model depends on the research question posed and how efficiently it can be addressed by the chosen technique and model. The application and availability of such models has been extensively reviewed [47,51].

Commonly, small and/or transparent animals are used to image surficial structures or structures well visible within their body for which purpose they are frequently adopted in developmental stud-

ies. *C. elegans*, drosophila larvae, and zebrafish embryos offer several key advantages as model systems in the study of physiological processes [52–57]. Optical transparency in combination with a broad toolset for genetic modifications (temporal and spatial controlled gene expression of fluorescent reporters) led to many novel insights into development and differentiation. Especially microscopic techniques such as light sheet microscopy allow for prolonged imaging with minimal direct interference with the imaged tissue.

Small rodents are very attractive models due to their genetic relation to human, short reproductive cycles, and availability of disease models. They are regularly used to study easily accessible organs, either superficially (i.e., skin, cornea) or through small incisions (i.e., abdomen, cardiovascular system, subcutaneous and surficial tumors). Adequate preparation of the tissue under study is a crucial step before exposing it to light microscopy imaging. This relates to the mechanical accessibility (e.g., the objective) as well as to the anatomical preparation of the tissue to be examined, especially in larger, non-transparent animal models. This is particularly challenging in IVM, since physiological and cellular processes in living organisms should not be influenced by preparation. Various preparation techniques have been developed (e.g., skin flaps, cranial/tissue windows, skinfold chambers, and surgically exposed tissues) to meet the requirements of IVM in living mice [58,59]. IVM has also been applied to awake mice under visual or haptic stimulation. For time-lapse imaging, special windows are installed on the skin surface, which allow the excitation light and signal to be transmitted without absorption by the skin or skull. These windows offer the possibility of imaging the same region at different time points, enabling longitudinal monitoring of the consequences of pharmacological or sensory interventions.

Modern IVM techniques rely on fluorescence detection. Labeling techniques using fluorophores facilitate the selective visualization of biomolecules, single cells, and cell populations, dynamic physiological processes, and even the development of entire organisms. The fluorescent signal can be endogenous or exogenous. The endogenous autofluorescence signal of tissues is often used for contrast. Transgenic animals offer attractive benefits, for which reason they are popular models for intravital imaging. Such animals are genetically modified to express a fluorescent protein (FP) at the site of interest, thereby adding specific, temporally and spatially controlled contrast. Direct labelling of the structures under investigations (e.g., proteins, organelles) with dyes is also possible, and they are typically based on direct interactions with biomolecules (i.e., synthetic fluorescent probes) or on antibody labeling (i.e., immunofluorescence). The application of the fluorophores to the region of interest often requires special preparation of the organism, e.g., intravenous injection of the solution with fluorescent probe in mice.

## 3. Imaging versatility: From small molecules to nanoparticles and from immune cells to the tissue microenvironment

IVM has substantiated itself as a powerful tool, distinguishing itself from other imaging modalities, due to its spatial accuracy at high temporal resolution. In the following section, we highlight the capability of IVM to visualize different levels of organization, extending from the visualization of metabolites, small molecules and nanoparticles, up to individual cells and components of the tissue microenvironment.

### 3.1. Imaging metabolites

The reprogramming of metabolism is one of the fundamental hallmarks of cancer [60,61]. Therefore, to understand carcinogenesis, metastasis and resistance to therapy, it is paramount to understand the mechanisms behind cellular energetics. Beyond cancer, also the pathogenesis of afflictions such as Crohn's disease or Alzheimer's disease [62,63] involve disruptions in energy metabolism. Apart from diseased states, understanding energy metabolism of regular biological systems, such as the energy balance of T cells [64], serves as a benefit in itself. Metabolic profiling is the leading tool to study the response of metabolites and their intermediates to various stimuli and grants scientists functional and physiological information on the state of cells and tissues.

In metabolomics, mass spectrometry (MS) and PET/MRI are the standard techniques used to study the ratio of glycolytic to oxidative metabolism. These techniques, though, either require sample destruction, they cannot provide dynamic information (MS), or they cannot achieve cell-level resolution (PET/MRI). IVM has been demonstrated to bridge the gap between these drawbacks. In a recent study, it was used to visualize the spatiotemporal correlation of glucose uptake and mitochondrial metabolism optically [65]. Through the use of IVM on dorsal window chambers in mice, near-simultaneous imaging of two molecules, namely 2-NBDG (fluorescent glucose derivate) and tetramethylrhodamine ethyl ester (TMRE; mitochondrial membrane potential) was achieved, which function as indicators of glucose uptake and mitochondrial membrane potential and activity, respectively. It was shown that TMRE intensity, under hypoxic conditions, decreases significantly as compared to normoxic conditions (Fig. 2**A**). Contrarily, under comparable conditions, 2-NBDG signal intensity increases (Fig. 2**B**). Interestingly, both TMRE and 2-NBDG showed an increased intensity compared to healthy tissue in the 4T1 triple negative breast cancer (TNBC) mouse model, indicative of a distinct metabolic pattern.

In an early account, metabolic imaging by means of intravital MP-FLIM was applied to hamster cheek pouch models for oral carcinogenesis, in order to investigate the benefit of such a system for

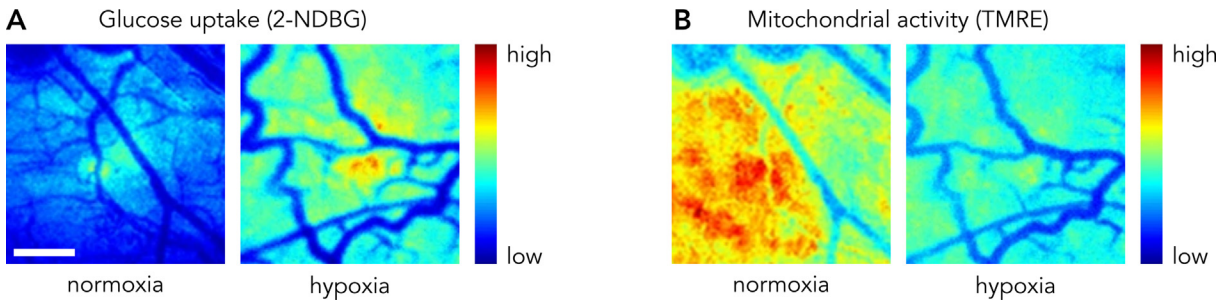


**Fig. 2. IVM visualization of metabolites. (A)** Spectral IVM heat map of relative glucose analogue (2-NDBG) uptake and distribution in normoxic or hypoxic tissue, revealing increased uptake under hypoxic conditions. Conversely, **(B)** uptake of the mitochondrial membrane potential probe TMRE decreased in the hypoxic tissue. All images were adapted with permission [65].

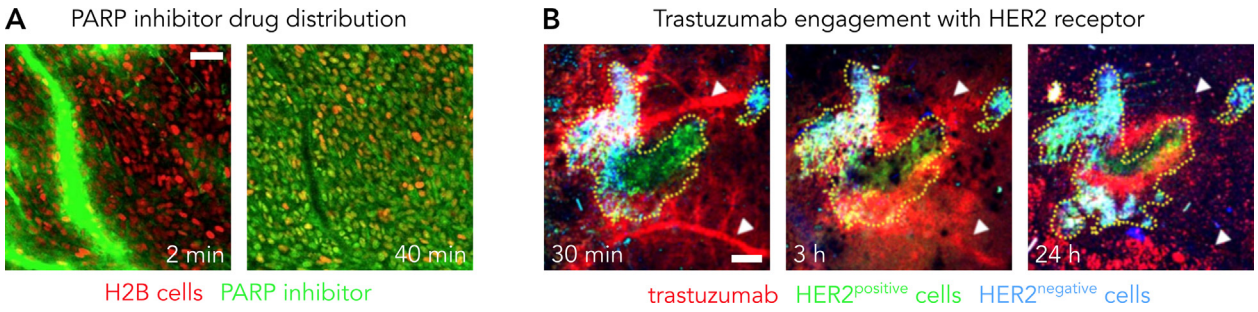


**Fig. 3. IVM visualization of small molecules and macromolecules. (A)** Rapid extravasation of fluorescent PARP inhibitor following complete perfusion of the tumor vasculature. The extravasated PARP inhibitor (green) initially bound non-specifically to the tumor tissue (H2B-RFP, red). However, non-specific accumulation was cleared over time, leaving only PARP inhibitor specifically bound to the nucleus of H2B cells. **(B)** Time lapse IVM showed trastuzumab (red) perfusion in the tumoral vasculature 30 min p.i. After 3 h, a substantial fraction of trastuzumab had already entered the tumor around the periphery of nearby blood vessels. After clearance of unspecifically bound drug, intratumoral signals for trastuzumab were shown to decrease after 24 h, with the residual drug being more significantly co-localized with HER2 receptor positive cells (green). All images were adapted with permission [70,74]. (For interpretation of the references to color in this figure legend, the reader is referred to the web version of this article.)

the *in vivo* detection of epithelial dysplasia [66]. The technique provided structural and metabolic information, which was used to discern healthy from dysplastic tissue *in vivo*. By exploiting the premise of the Warburg effect, and considering the tendency of neoplasia to switch from oxidative phosphorylation to glycolysis under anaerobic conditions [67], dysplastic tissue was differentiated based on the NADPH redox state. The redox ratio of NADPH is highly dependent on and can be shifted by the inhibition of either glycolysis or oxidative phosphorylation.

While the data analysis of FLIM imaging can pose a significant challenge [68], methods have been explored to circumvent this. Through phasor plot transformation of FLIM data, identification of distinct fluorescence lifetime values is made possible [69]. These data were subsequently used to differentiate between functionally distinct kidney structures, such as the proximal tubules S1 and S2, and resolve structures not discernable from intensity contrast alone. This demonstrates that structures can be distinguished with relative ease and considerable confidence, in terms of their metabolic microenvironment using intravital FLIM.

### 3.2. Imaging small molecules and macromolecules

IVM's excellent temporal resolution at high spatial resolution has been exploited to study the distribution and target-binding of drugs. In this regard, IVM was used to monitor in real-time the distribution of an olaparib-based fluorescent poly (ADP ribose) polymerase (PARP) inhibitor (PARPi). Olaparib is a PARP inhibitor commonly used in the clinic for the treatment of advanced BRCA-mutated ovarian cancer. The rapid extravasation of fluorescent PARPi was demonstrated after complete perfusion of the functional tumor vasculature, distributing non-specifically in histone-H2B-RFP expressing cells. While target binding occurred promptly, non-specifically bound PARPi cleared within the first hour post injection, demonstrating optically the specificity of PARP target binding by the Olaparib-analogue *in vivo* (Fig. 3**A**) [70,71]. In a similar manner, the cellular pharmacokinetics and tissue distribution of a fluorescent eribulin analogue was analyzed using IVM [72]. Eribulin is a cytotoxic drug developed to treat taxane-resistant cancers, however, for reasons yet unknown, it does not work in a subset of patients. By assessing the cellular PK of cytotoxic drugs such as eribulin using IVM, it is postulated that mechanisms of drug resistance can be determined, leading to the discovery of novel strategies to tackle resistance. Here it was discovered that the efflux of the eribulin analogue and therefore eribulin resistance relied on the expression and activity of multidrug resistance protein 1 (MDR1).

The development of resistance to chemotherapy is one of many challenges encountered when treating cancer. Most research on how the microenvironment influences the development of drug resistance examines the resistance behavior under *in vitro* or xenograft conditions. While *in vitro* approaches are valuable, IVM allows for the visualization of treatment outcome *in vivo*. In an effort to elucidate the microenvironmental response of progressive cancer upon chemotherapy, a mammary tumor virus (MMTV), promoter-driven polyoma middle T oncogene murine model was studied using IVM. Intravital imaging revealed that sensitivity to doxorubicin was dependent on tumor stage and that cancer cell proliferation is not a comprehensive indicator for drug sensitivity. On the contrary, drug distribution was suggested as a superior marker of drug sensitivity [73].

Transitioning from small molecules to macromolecules, a robust example involved the use of confocal IVM to investigate the pharmacology of the therapeutic monoclonal antibody trastuzumab, a treatment for breast and gastric cancer, in a mosaic xenograft tumor mouse model which variably expresses the HER2 receptor [74]. As trastuzumab targets HER2, the increased accumulation in HER2-overexpressing cells compared to HER2-deficient cells came to no surprise. However, the majority of drug distinctly accumulated in tumor-associated phagocytes, achieving 80% accumulation after a period of 48 h post injection. The extravasation of trastuzumab from the vasculature to the tumor interstitium as well as the quantification of its subsequent clearing was demonstrated specifically via IVM (Fig. 3**B**).

### 3.3. Imaging nanoparticles

A key advantage of IVM is the ability to conduct multichannel imaging with adequate spatiotemporal resolution. This facilitates the tracking of nanoparticle tissue distribution, thus providing an option to simultaneously visualize parts of the tissue microenvironment as reference (e.g., blood vessels) [7].

Pharmacokinetic analysis of therapeutic nanoparticles was conducted [75], utilizing time-lapse confocal IVM in a dorsal window chamber model of HT1080 xenograft tumor models expressing a fluorescent protein labeling the nucleus. The research demonstrated the possibility of tracing the distribution of both nanoparticles and payload (Fig. 4**A**). Likewise, the capacity of IVM to distinguish the more gradual and reduced nanoparticle uptake of cancer cells compared to the perivascular cells of the host was displayed. Furthermore, by labeling tumor-associated macrophages (TAMs) with fluorescent dextran-coated nanoparticles, the authors

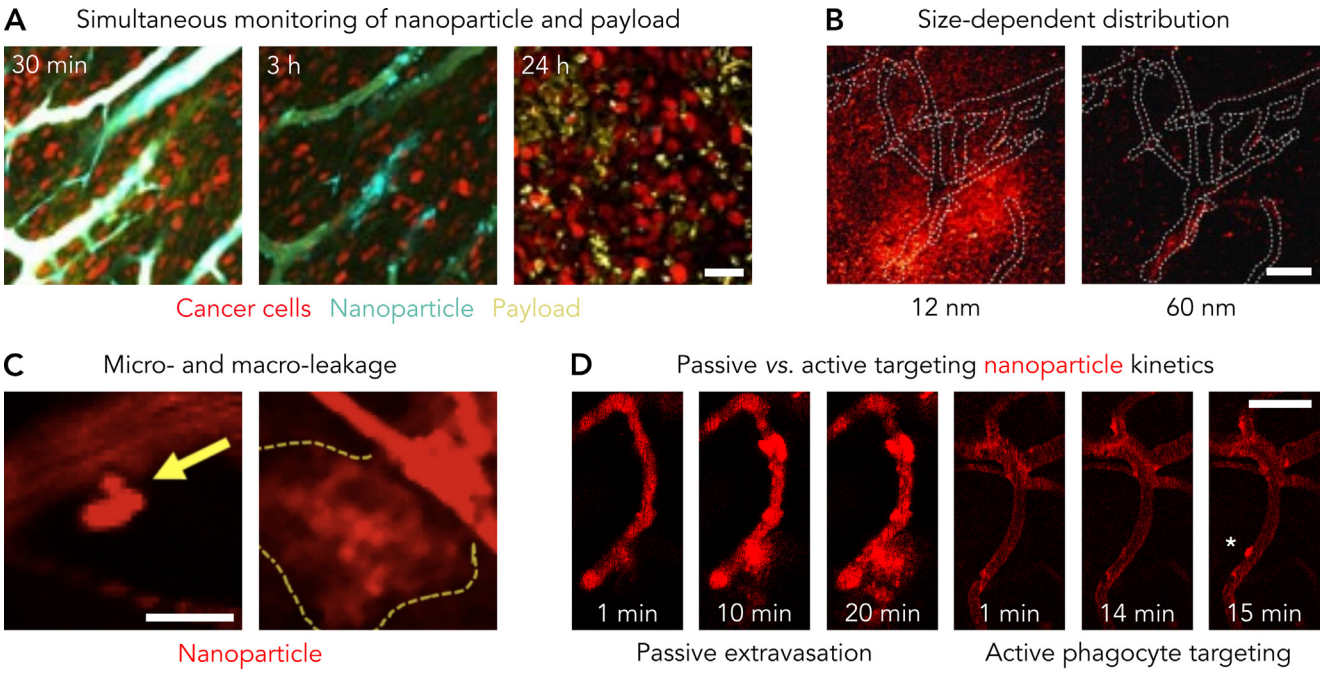


**Fig. 4. IVM visualization of nanoparticle distribution and targeting kinetics.** **(A)** Time-lapse confocal IVM of microvasculature half-life and tissue accumulation of therapeutic nanoparticles (cyan) and payload (yellow) in a dorsal window chamber model of tumor cells expressing fluorescently tagged 53BP1 (red). Initially, the loaded TNP co-localized significantly to the microvasculature while a fraction of the payload extravasated into the tissue independently from the nanoparticle. After 3 h, extravasated payload had been cleared, while TNPs continued in circulation. At 24 h, the TNP was no longer in circulation, though the payload has accumulated heterogeneously within the tissue. **(B)** MP-IVM of size dependent nanoparticle (red) distribution in a dorsal skinfold chamber model of mU89 melanoma bearing mice. The 12 nm NP had extravasated heterogeneously though at a much greater rate as compared to the 60 nm NP. The larger nanoparticle, by contrast, showed only minimal extravasation within the immediate perivascular space. White, dashed lines indicate the position of the vasculature. **(C)** Two distinct extravasation patterns by fluorescent liposomes (red), in a 4T1 orthotopic tumor model, termed microleakage (left panel) and macro-leakage (right panel). The more frequent microleakage (yellow arrow) is characterized by a confined spread. Macro-leakage (yellow dashed line) was shown to spread much further and more diffuse into tissues. **(D)** Co-administration of passive and active-targeting nanomedicines (i.e., control and cRGD-decorated liposomes) in a wound-healing inflammation model, shows the first to diffuse through vasculature, and the latter to hitchhike in the vasculature with phagocytes (star "*"). All images were adapted with permission [75–78]. (For interpretation of the references to color in this figure legend, the reader is referred to the web version of this article.)

demonstrated significant co-localization of therapeutic nanoparticles with TAMs.

A study investigating a size series of nanoparticles (10–150 nm), determined the dependency of nanoparticle distribution in solid tumors on particle size using multiphoton laser-scanning IVM [76]. Smaller nanoparticle size resulted in improved distribution and penetration depth, as validated through penetration depth analysis (Fig. 4**B**). This work illustrates the benefit of IVM in a real-time set-up and meaningfully demonstrated the importance of nanoparticle size in its tumor accumulation properties.

In addition to visualizing and timing nanoparticle accumulation, IVM allowed for the discovery of more complex extravasation patterns by which nanoparticles (e.g., liposomes) extravasate in different xenograft tumor models as well as healthy skin tissue [77]. These patterns have been coined microleakage and macroleakage. Macro-leakage is characterized by a rapid formation of extensive egress, while microleakage is defined as focused and localized egress of liposomes (Fig. 4**C**). It is shown that microleakages, which occur primarily around the vasculature of both tumor and healthy tissue, do not seem to result in nanoparticle distribution to cancer cells. Contrarily, macro-leakages grant for deeper penetration depths into the tumor. It is hypothesized that shifting the extravasation pattern from microleakage to a macro-leakage-dominated one, could facilitate drug delivery. Of note, the significance of neutrophil extravasation (i.e., very motile immune cells with high tumor infiltration properties) on both macro-leakage and microleakage was demonstrated, as it was revealed that neutrophil extravasation is accompanied by liposomal extravasation.

A follow-up study investigating the kinetics of passively and actively targeted liposomes and oil-in-water nanoemulsions in a wound-healing inflammation model revealed a difference in the extravasation patterns between control and cRGD-decorated analogues. Specifically, co-injection of passively and actively targeted nanoparticles showed the control formulation to extensively extravasate from specific spots on the vasculature (resembling micro/macro-leakage), while the active targeting formulation formed "clusters" in the circulation that later migrated to angiogenic endothelium (Fig. 4**D**). This high-resolution IVM (temporal resolution of 256 ms), together with ex vivo microscopy and flow cytometry, revealed these "clusters" to be cRGD-nanoparticles taken up by circulating myeloid cells [78].

Furthermore, imaging using MP-IVM has demonstrated the high frame-rate visualization and tracking of unlabeled gold-nanoparticles (AuNPs) within the unperturbed, *in vivo* vascular environment [79]. The employed method exploits the inherent contrast of intrinsic luminescence induced via multiphoton absorption by AuNPs as well as second harmonic generation and autofluorescence of the vasculature, thus absolving the use of exogenous labeling. Currently, examination of NPs' circulation half-lifes by means of sequential blood draws (analyzed by induction coupled plasma mass spectrometry) is a standard method for the visualization of NPs *in vivo* [80,81].

### 3.4. Imaging immune cells

IVM has granted remarkable insights into immune cell dynamics [82]. It is currently the sole real-time method for investigating inter- and intracellular events *in vivo*.

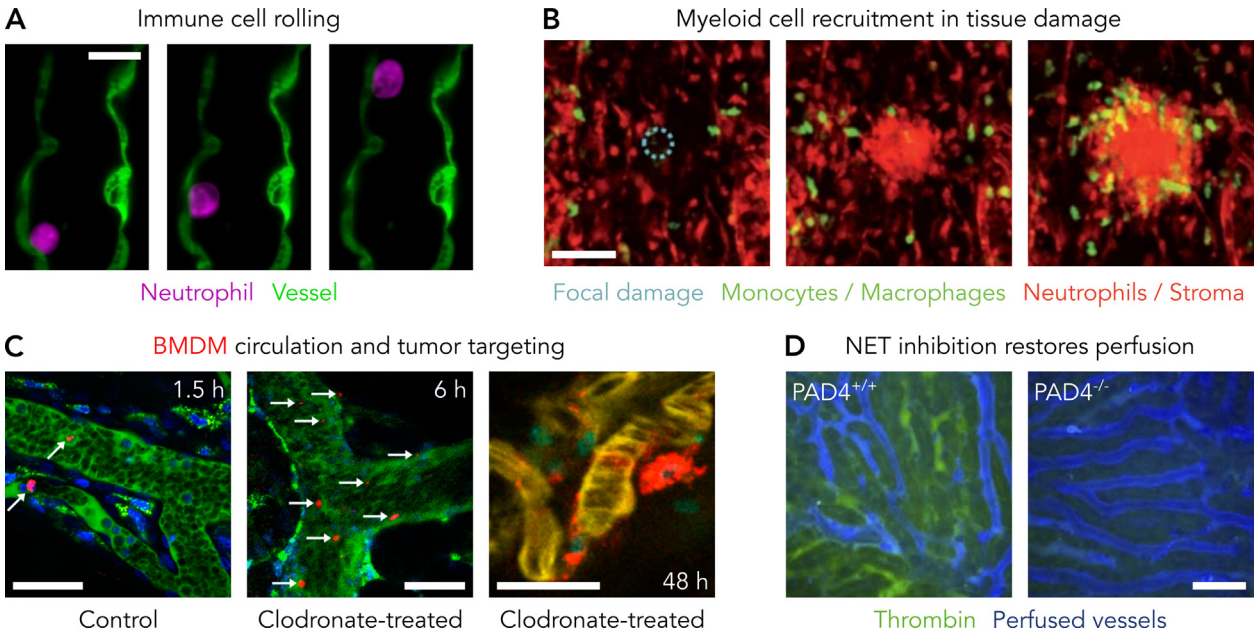


**Fig. 5. IVM visualization of endogenous and administered immune cells. (A)** Intravital single-plane LLSM, at 200 frames per second, showing rolling of a neutrophil (magenta) on the vascular endothelium (green) in zebrafish. **(B)** Multiphoton IVM of the murine ear demonstrated interstitial neutrophil (red) and monocyte (green) recruitment on sites of focal injury (blue dashed circle), as inflicted via two-photon laser. Neutrophils were shown to immediately localize and accumulate at the site of injury. Monocytes/ macrophages tended to accumulate much later and only at the periphery of the earlier formed neutrophil/ stroma complex. **(C)** Depletion of the mononuclear phagocyte system via clodronate treatment significantly prolonged circulation and increased the accumulation in the tumor interstitium of administered BMDM. **(D)** Spinning disk confocal IVM of the liver microcirculation in an intravascular coagulation model showed the impaired perfusion (blue) of vessels (thrombin, green) in wildtype ($PAD4^{+/+}$) mice. In PAD4-deficient mice, perfusion remained unaffected by the coagulation model, likely due to the failure of neutrophil extracellular trap formation. All images were adapted with permission [83,85–87]. (For interpretation of the references to color in this figure legend, the reader is referred to the web version of this article.)

A study on leukocyte dynamics has introduced the benefits of lattice light sheet microscopy (LLSM) to the immune cell physiology in zebrafish, allowing for the visualization of dynamic processes and morphological changes of leukocytes proximally to the vasculature. LLSM imaging captured the swift rolling of neutrophils along the luminal wall at 200 frames/second (Fig. 5**A**). LLSM has shown to capture rapidly moving neutrophils, uropod extension during interstitial migration, and formation of lamellipodia by intravascular neutrophils [83]. Such IVM observations are valuable considering that intravascular neutrophils are known to form fine, elongated membrane protrusions, which function as tethers to the stationary environment in order to stabilize or halt their rolling motion [84].

In an effort to investigate actively targeted nanoparticle extravasation kinetics, high-speed dynamic IVM granted the visualization of free cRGD-nanoparticles traveling fast across the field of view, or taken up by and traveling together with circulating phagocytes. Nanoparticle-targeted immune cells were seen to roll along the vascular lumen, and halting their motion when encountering an already stationary phagocyte attached to the vascular lumen [78]. In a similar set-up, IVM allowed the visualization of neutrophil extravasation that consequently contributed to nanoparticle leakage [77].

Interested in the signaling-specific neutrophil recruitment in tissue damage, a study demonstrated the role of leukotriene B4 and integrin in the neutrophil swarming dynamics [85]. The coordination of neutrophil swarming towards sites of injury was observed using MP-IVM following two-photon induced focal and sterile skin injury on the murine ear. Neutrophils were shown to chemotax efficiently through the interstitial space and cluster at the injury site upon which the recruitment halts. Macrophages showed divergent behavior with slower migration speeds and only performed chemotaxis towards the site of injury after the formation of the neutrophil cluster, eventually cumulating on its periphery (Fig. 5**B**).

In addition to the observation of endogenous immune cell behavior, administration of exogenous bone marrow-derived monocytes (BMDMs) was monitored via confocal IVM in order to investigate their applicability as "chariots", i.e., ex vivo cargo loading and subsequent tumor delivery. It was shown that BMDMs migrated vastly in the tumor microenvironment when the endogenous phagocytes where depleted via liposomal clodronate [86]. The visualization of exogenous BMDMs was achieved via DiD and Hoechst double-labeling and facilitated by co-injecting the endogenous-tumor associated macrophage tracer tetramethylrhodamine labeled 40 kDa dextran (Fig. 5**C**).

While ex vivo analysis and blood sampling has provided invaluable insights into the involvement of coagulation and the immune system ensuing sepsis, *in vivo* imaging is mandatory for monitoring the dynamic processes in the sepsis microenvironment. Spinning disk and resonance scanning confocal intravital microscopy in combination with fluorescently labelled thrombocytes revealed the dependence of microvascular dysfunction and organ damage on a neutrophil extracellular traps (NET)-platelet-thrombin axis in sepsis (Fig. 5**D**) [87].

### 3.5. Imaging the microenvironment

Our definition of cancer has evolved from dysregulated cellular proliferation to also include intricacies in the tumor microenvironment (TME) [73,88-90], which comprises of cancer, endothelial, stromal, and immune cells, as well as the extracellular matrix [91,92]. The TME is characterized by a milieu of distinctive cellular and acellular components and their interactions. Although *ex vivo* and *in vitro* analyses offer important insights, they are limited due to the absence of dynamic information. In this regard, IVM

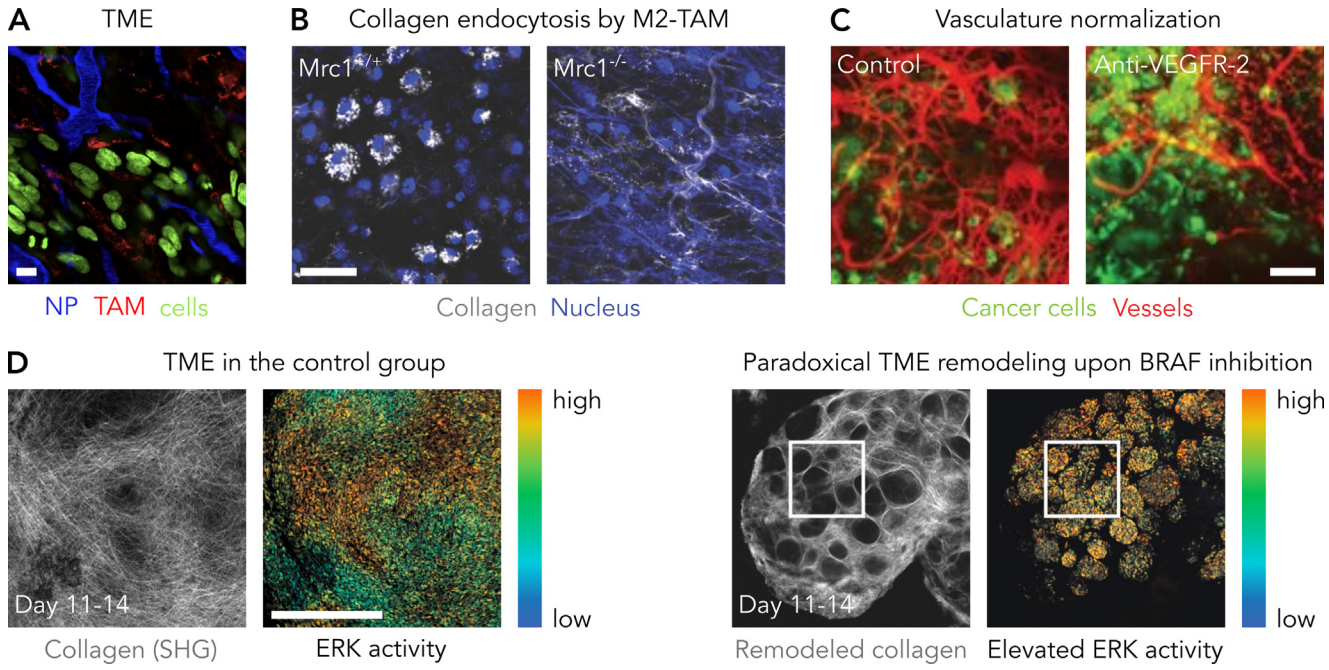


**Fig. 6. IVM visualization of cells, vessels, and extracellular matrix in the TME. (A)** IVM was utilized simultaneously for visualizing cancer cells (green), the vasculature (blue) and TAMs (red) in separate channels, demonstrating its capability to image and track the interactions of the different TME components, relevant to nanoparticle delivery. **(B)** IVM of Lewis lung carcinoma in mannose receptor (MR) expressing as well as MR deficient mice illustrated the mannose receptor mediated endocytosis of collagen (white) by tumoral cells (nuclei, blue). Fluorescent collagen in MR expressing mice was shown to co-localize with macrophages, unlike in MR deficient mice, where collagen was diffusely distributed throughout the observed tissue. **(C)** Intravital imaging of an orthotopic GL261 glioma (tumor cells, green) demonstrated vessel normalization upon anti-VEGFR-2 treatment. Treatment improved the tumor vasculature (dextran, red) by reducing vessel tortuosity and density. **(D)** FRET imaging of an ERK-biosensor and two-photon second harmonic generation of collagen in orthotopic melanoma revealed BRAF-independent ERK activation and 'paradoxical' TME remodeling following BRAF inhibition. ERK activity was elevated following 11–14 days of BRAF inhibition and melanoma cells co-localized with niches in the remodeled collagen structure, as compared with the DMSO-treated control. All images were adapted with permission [93-96]. (For interpretation of the references to color in this figure legend, the reader is referred to the web version of this article.)

has introduced its capacity of multichannel *in vivo* imaging to the study of the TME.

The first important benefit of IVM is the simultaneous imaging of key components of the TME. Intravital imaging of the TME has shown its potential to visualize the three primary components of the TME for NP delivery: tumor cells, tumor-associated macrophages, and the vasculature [93]. The TME can be easily imaged at the scales of cells as well as tissues, while simultaneously visualizing the abovementioned components in three separate channels (Fig. 6**A**).

The visualization of the extracellular matrix (ECM) and its remodeling can be highly complementary to the sole visualization of cells. In a subcutaneous Lewis lung carcinoma in syngeneic wild type and mannose receptor deficient mice, fluorescent collagen was injected to ascertain the function of mannose receptors in the endocytic collagen degradation in tumors [94]. Imaging and subsequent analysis discovered that a number of cells were capable of performing endocytosis of the injected collagen in mannose receptor expressing mice, while hardly any cells were engaged in the same process in mannose receptor deficient mice (Fig. 6**B**). In concurrence with these IVM images and by combining imaging with flow cytometry, the significance of TAMs in the interstitial degradation of collagen was demonstrated; thus, further highlighting the role of TAMs in the remodeling of the extracellular matrix of the TME.

Another significant advantage of IVM is the ability to swiftly detect changes upon treatment at the tissue/cellular resolution. In an effort to visualize vascular normalization in the brain tumor tissue upon treatment with an anti-VEGFR-2 antibody (DC101), MP-IVM was employed on DC101-treated mice bearing orthotopically implanted GL261 glioma [95]. A reduction in blood vessel 4tortuosity and density became evident after treatment with the anti-VEGFR-2 antibody in comparison to the control group (Fig. 6**C**). Close inspection of the vasculature revealed a gradual increase in pericyte coverage, which constituted to a decrease in vascular egress.

In an effort to investigate the rapid progression of BRAF inhibitor (PLX4720) tolerance of melanoma cells, IVM of a FRET-biosensor (EKAREV) for BRAF activity through monitoring of the ERK/MAPK signaling pathway was used to evaluate the response of tumor stromal distribution to BRAF [96]. It was observed that, although two melanoma models (A375 and WM266.4) exhibited sensitivity for PLX4720 treatment at first, a residual tumor mass remained throughout the duration of treatment. Based on results from preceding experiments, it was hypothesized that stromal changes may provide protection from treatment to the otherwise sensitive residual tumor cells. The answer was revealed through IVM of the FRET-biosensor, which established that the post-treated, residual tumors have shown comparable levels of ERK activity to the same tumors prior to treatment. This indicates BRAF-independent ERK activation. Furthermore, significant remodeling of collagen was observed upon treatment with PLX4720 as indicated by second harmonic generation (SHG) imaging, when compared to the non-treated group (Fig. 6**D**).

In the elucidation of the TME, both multiphoton and confocal IVM have been extensively used. A comparative analysis of two microscopy modalities, confocal and multiphoton microscopy, has compared and contrasted these modalities for IVM use in intramuscular tumors by capturing a common field of view between the two [97]. Both platforms grant adequate visualization of the vasculature, cells and overall topography. This is done through the utilization of a computer driven microscope stage which allows for the capture of several fields of view that together form a mosaic image. Due to rapid acquisition speeds, the complete mosaic can

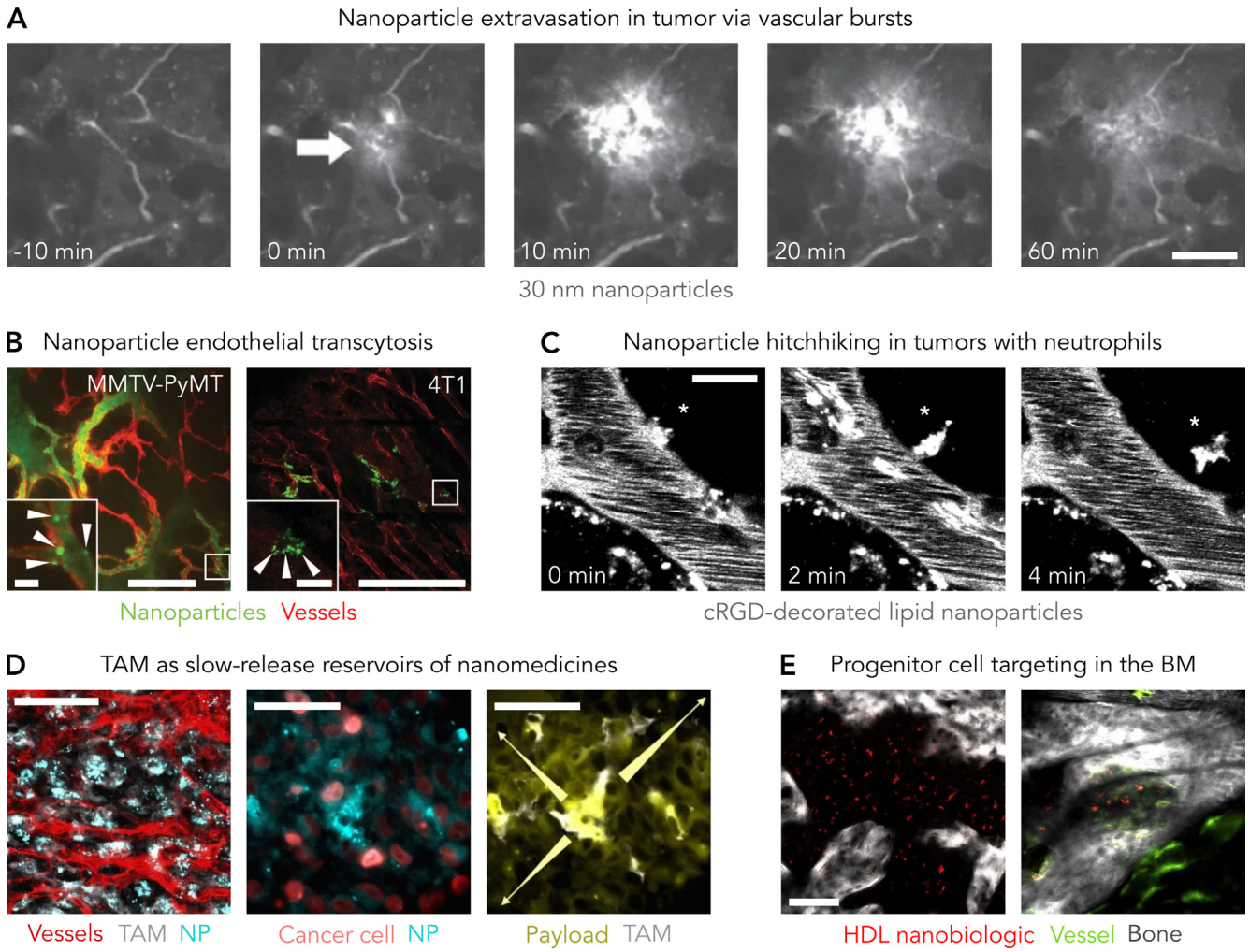


**Fig. 7. Investigating nanoparticle targeting mechanisms and targeting kinetics with IVM. (A)** Intravital CLSM of an orthotopic BxPC3 tumor showed individual bursts of 30 nm NPs from the vasculature. The bursts were shown to occur transiently and unpredictably throughout the tumor vasculature. The 0 min time point marks the initiation and the white arrow indicates the position of the vascular burst. **(B)** Intravital spinning disk confocal microscopy in MMTV-PyMT and 4T1 tumors demonstrated co-localization of gold nanoparticles (green) with the vasculature (red), leading to suggest nanoparticle extravasation via a transcytosis pathway. The formation of nanoparticle hotspots on the vessel lumen was observed, as indicated by the white arrowheads. **(C)** Intravital CLSM of a TNBC orthotopic mouse model reveals active targeting nanomedicine to occur via hitchhiking with circulating phagocytes. Specifically, cRGD-decorated lipid nanoparticles are taken up my circulating phagocytes (especially neutrophils), which dynamically penetrate through the endothelium, extravasating to the TME. **(D)** Imaging of lung tumor cells in an Cx3cr1GFP$^{/+}$ reporter mice revealed increased therapeutic nanoparticle uptake by host TAMs (white), as indicated by the co-localization of nanoparticles with TAMs. Imaging of an HT1080-mApple tumor model, demonstrated an increased payload (yellow) concentration in close proximity to TAMs. **(E)** MP-IVM of B16F10 tumor bearing mice 8 h post injection with an HDL nanobiologic and fluorescent dextran (vasculature, green) showed clear uptake of HDL nanobiologic (red) with myeloid cells of the calvarium bone marrow (white). All images were adapted with permission [75,104,107,110,116]. (For interpretation of the references to color in this figure legend, the reader is referred to the web version of this article.)

be imaged several times in short time intervals (sub-second range) composing, in essence, a relatively high framerate video. Between the two modalities, multiphoton derived images allowed for more visualization at higher depth (800 μm for MPM as compared to 150–200 μm for confocal), and therefore a more detailed 3D TME representation.

Additionally, intravital microscopy has expanded our understanding of the blood brain barrier (BBB) and the exploitation thereof for drug delivery purposes. Albumin, for example, has been considered as a potential companion diagnostic or even as a theranostic tool in the delivery of drugs across the BBB. The ratio of albumin levels in the blood and the cerebrospinal fluid can be utilized to assess the integrity of the BBB. Recently, fluorescent labelling of albumin in mouse models for cerebrovascular accidents has allowed for both visualization of bovine serum albumin (BSA) transport across the BBB [98]. In a different study, IVM through cranial window implementation, coupled with flow cytometry visualized the pharmacodynamics and pharmacokinetics of a nanocarrier-conjugated antibody [99]. It was demonstrated that the liposomal anti vascular cell adhesion molecule 1 (anti-VCAM) interacted with the endothelium rather than with leukocytes, in the inflamed brain tissue. Besides, two photon and three photon microscopy of the BBB enables the *in vivo* study of its endothelial barrier, allowing for the real time examination of its structural and functional aspects.

## 4. Visualizing new nanoparticle targeting mechanisms

Many nanoparticle targeting processes can be described as dynamic and short-lived events. Cell-nanoparticle interactions within the bloodstream, by nature, are mostly transient occurrences, demanding *in vivo* imaging techniques with emphasis on high spatiotemporal resolution [100]. When studying processes of drug delivery, in particular, IVM has facilitated the discovery

of novel targeting mechanisms. The following subsections will give examples of how IVM has allowed for the study of various drug delivery processes in unprecedented detail, and extend our understanding on nanoparticles targeting kinetics and mechanisms [100].

### 4.1. Vascular bursts

Traditionally, the retention of nanomedicines in solid tumors was described as a homogeneous extravasation of nanomedicines from the leaky and pericyte-deprived tumor vasculature [101,102]. With time, evidence had emerged demonstrating uncertainty of the clinical relevance of the above phenomenon [103]. Deviating from this static view of passive drug delivery, a recent account has utilized IVM to extend our understanding and reveal a rather dynamic process instead.

By utilizing intravital laser scanning confocal microscopy (IV-LSCM) on hypovascular human pancreatic BxPC3-GFP tumors implanted in BALB/c nu/nu mice, a phenomenon referred to by the authors as vascular bursts was revealed [104]. By this mechanism, vascular bursts accompanied by transient eruptions translocate fluids into the tumor environment (Fig. 7**A**). It was further demonstrated that NPs below 30 nm in size make use of static pores and eruptions alike, while NPs approximately 70 nm in size are translocated to a greater extent via eruptions. Separately, high resolution intravital imaging, following local tumor irradiation, has reported TAM elicited dynamic bursts of extravasation and a resultant increase in drug uptake by adjacent tumor cells [105].

Another study concluded that such vascular eruptions can also be extensive and local, described as macro- and microleakages, respectively, and occur in correlation with the extravasation of neutrophils [77]. Further investigation demonstrated the relevance of vascular bursts in the delivery of liposomes and has hypothesized about the significance of a porous vasculature in the accumulation of liposomes in healthy skin tissue, albeit conflicting inferences, in which endothelial transcytosis is suggested as the predominant mechanism [106].

The nature of these dynamic, vascular eruptions implies the possible extravasation of even larger NPs into the tumor interstitium, where the lack of mobility, though, impedes deep tumor penetration.

### 4.2. Endothelial transcytosis

Diverging from the current paradigm of drug delivery mechanisms, an alternative mechanism of NP transport into solid tumors is being proposed. Majorly investigated via electron microscopy, evidence for an alternative process to vascular bursts or leakage through vasculature pores, suggested the delivery of nanoparticles into solid tumors to occur primarily via endothelial transcytosis. Intravital micro-lensed spinning-disk confocal microscopy across two murine tumor models corroborated the transmission electron microscopy (TEM) data, supporting the process of endothelial transcytosis as mechanism of extravasation for PEGylated gold nanoparticles (Fig. 7**B**). Furthermore, computational analysis coupled with 3D imaging and TEM indicated inconsistencies between observed gap frequency and measured tumor nanoparticle accumulation. Taken together, these results suggest passive drug delivery processes to confer a less significant role than active processes [107], at least for the inorganic nanoparticles investigated in this study.

Nonetheless, a more detailed intravital microscopy of the observed focal nanoparticle hotspots on the endothelium is needed to serve as corroborative evidence for endothelial transcytosis. This includes investigating the potential involvement of immune cells and explicitly demonstrating an interaction of these hot spots with endothelial cells.

### 4.3. Hitchhiking with immune cells

Active targeting to the tumor by nanomedicines (i.e., targeting of a specific receptor) provides an attractive concept for drug delivery. Nanoparticles demonstrated to actively target certain tumors selectively, for example, are currently being investigated for clinical use [108,109]. To examine the complex *in vivo* behavior of these novel active targeting approaches requires means of real-time *in vivo* elucidation, as can be offered by intravital imaging.

In a recent study, IVM (combined with *in vivo* PET/CT imaging, flow cytometry, ex vivo microscopy, and histology) was used to study the fate of two lipid nanoparticle platforms targeting $\alpha_v\beta_3$-integrin through a cyclic arginine-glycine-aspartate (cRGD) ligand [110]. It was discovered that targeting of active cRGD-decorated nanoparticles to the tumor vasculature is facilitated by the phagocytic hitchhiking of these nanoparticles (Fig. 7**C**). Furthermore, it was shown that phagocytes had extravasated into the tumor and, in the process, distributed the internalized nanoparticles. Flow cytometry data corroborated the extensive engagement between nanoparticles and phagocytes, and especially neutrophils. In an earlier account, IVM had enabled the discovery of RGD-decorated single-walled carbon nanotubes uptake by circulatory monocytes [111].

Following the discovery of cRGD-nanoparticle uptake by circulating phagocytes and subsequent tumor homing, the process was studied in an inflammatory setting [78]. In an acute wound-derived inflammatory murine model, IVM (complemented with *ex vivo* microscopy and flow cytometry) revealed a similarly targeted phagocytic hitchhiking of decorated NPs to inflammatory regions. Despite the mechanistic similarities to the tumor-homing hitchhiking, targeting to inflamed tissues occurred comparatively organized. On top, the nanoparticle-loaded phagocytes displayed an extensive vasculature homing in comparison to cancer, where their extensive extravasation to the malignant tissue was recorded. Similarly, an earlier study has shown, using IVM, the *in situ* targeting of activated neutrophils by bovine serum albumin NPs and the subsequent extravasation into inflammatory lesions in the lung [112].

To elucidate the extravasation kinetics of various nanoparticles as well as to monitor the different engagement with circulating phagocytes, IVM can be supported through antibody labeling [113]. Here, an approach for an MRI-based liposomal companion drug is discussed. It was validated, using intravital confocal microscopy that the loading with maghemite nanoparticles and a therapeutic payload did not interfere with the biodistribution and extravasation behavior of liposomes, as well as its interactions with immune cells *in vivo*.

In light of the presented active targeting mechanisms via immune cell hitchhiking, a clear demand is shown for an improved understanding of nanoparticle behavior *in vivo*. Further study of this phenomenon may facilitate a rational approach for the application of nanomedicines by uncovering the interactions between immune cells and NPs. This could potentially be exploited for the development of novel immunotherapies.

### 4.4. Macrophages as nanoparticle reservoirs

The study of nanoparticle *in vivo* behavior primarily focuses on targeting mechanisms, with the goal to achieve enhanced permeability in the targeted tissues. However, another very important field of interest centers around the identification of mechanisms that result in high retention of nanomedicines in malignant

regions, this concept has been traditionally attributed to lymphatic impairment.

In a study employing intravital TPLSM in tumor-bearing mice, two model therapeutic nanoparticles (TNPs) were investigated for their pharmacokinetic and immune cell interactions. Here, a platform was created that has enabled the simultaneous intravital imaging of 100 nm nanocarriers and their therapeutic payload, and in the process visualized therapeutic outcome at the cellular level. This work implicated tumor-associated macrophages as cellular drug reservoirs, by demonstrating an increased accumulation of TNP in these immune cells. Progressively, the nanoparticle payload seemed to diffuse from TAMs towards the surrounding tissue, revealing the TAMs to act as slow-release reservoirs (Fig. 7**D**). This potentially shifts the focus from nanoparticle retention by lymphatic drainage away to retention by TAMs [75].

Time-lapse intravital confocal microscopy in a tumor and immune cell specific fluorescent reporter mouse model has shown the potential involvement of TAMs in immune checkpoint blockade therapy (aPD-1 mAb) [114]. While co-localization of aPD-1 mAb with cytotoxic T cells was visualized as expected, further imaging of drug pharmacokinetics revealed the reduction of labelled T cells via the transfer of antibody from T cells to TAMs, despite their inability to accumulate the free antibodies in circulation.

The presented paradigm of TAMs as slow-releasing reservoirs may prove beneficial in the development and translation (i.e., patient stratification based on peritumoral TAM content) of TNPs in the future. Furthermore, IVM enables to further study this principle in the context of therapies that modulate (increase or decrease) TAM content [73,115].

### 4.5. Targeting cells in hematopoietic organs

The innate immune system, contrary to our previous understanding, is shown to exhibit long term memory, labeled as trained immunity mediated by metabolic and epigenetic alterations. The regulation of trained immunity occurs through the functional reprogramming of myeloid cells.

Recently, nanoimmunotherapeutic targeting of the bone marrow was shown to elicit trained immunity, suppressing tumor growth, while modulating the susceptibility of the immune system to checkpoint blockade therapy [116]. Here, intravital microscopy revealed associations of nanoparticles with myeloid cells of the spleen as well as the calvarium bone marrow, suggesting nanoparticle uptake by these structures. SHG in the bone marrow visualized bone structures, while in the spleen and the tumor it uncovered the collagen structure. Additionally, TAMs near the tumor vasculature were found to accumulate nanoparticles and the internalized dextran allowed for their delineation from the vasculature (Fig. 7**E**).

Complementary to the IVM, flow cytometry, gating for bone marrow, spleen and the tumor, was used to dissect the nanoparticle accumulation amongst different subsets of immune cells in these tissues. Increased uptake was shown for hematopoietic stem cells (HSCs) and multipotent progenitors (MPPs) in all measured tissues. However, for each tissue, lymphocytes only showed minimal uptake. By the combinatory use of IVM and flow cytometry, this study demonstrated the epigenetic rewiring of HSC and MPP cells and a robust and rapid system wide increase of myeloid cells caused by myelopoiesis, both of which are hallmarks of trained immunity.

## 5. Imaging complex and dynamic biological processes

Current advances in the field of microscopy as applied to intravital imaging have allowed for the investigation of even the most puzzling *in vivo* processes. This section will highlight different biological processes and show how each process has been characterized under the scrutiny of IVM.

### 5.1. Cell death of immune cells

Although the vast majority of imaging-derived knowledge stems from *in vitro* and *ex vivo* studies [117–121], recent studies attempt to visualize cell death *in vivo* using IVM. The bulk of intravital microscopy has visualized cell death by staining the observed tissue with markers of cell death (i.e., propidium iodide) or exploiting the benefits of FLIM or FRET microscopy [122–125].

Capitalizing on the high spatiotemporal resolution of LLSM, the immobility, nuclear fragmentation and subsequent clearing by adjacent phagocytes of neutrophils in living tissue had successfully been visualized (Fig. 8**A**). A stationary phagocyte with a hyper-segmented nucleus was shown to get recognized by neighboring phagocytes. The adjacent neutrophils appeared to clear out much of the cytoplasm and the entirety of the nucleus of the expiring neutrophil. It was deduced that the hyper-segmentation may present a feature of an unknown cell death pathway. However, neutrophil hyper-segmentation has been described as a common morphological feature of tumor associated neutrophils [126], as well as evidence for neutrophil heterogeneity during cell aging and disease [127,128] and may therefore be incidental. However, intravital LLSM bears potential to further investigate specific cell death pathways, by using applicable markers for candidate pathways of cell death.

In a different study, multi-laser spinning disk confocal IVM was utilized to examine the generation, persistence, and biological relevance of neutrophil extracellular traps (NETs) in bacteremia [129]. NET formation within the liver sinusoids from recruited neutrophils upon intravenous methicillin-resistant *Staphylococcus aureus* (MRSA) infection is associated with extensive liver injury, which was diminished through the inhibition of NET formation rather than clearance of DNA by DNAses.

Based on *in vitro* data, taxane-induced apoptosis was believed to occur due to aberrations of mitotic progression. However, research investigating drug-induced tumor cell death demonstrated that docetaxel-induced apoptosis does not necessarily occur through mitotic defects [124]. Using IV-MPM of caspase-3 Förster resonance energy transfer (FRET) probes and a histone-fused photo-switchable probe, progression of apoptosis was tracked, but was shown to not coincided with mitotic progression. This serves to exhibit the power of intravital imaging to enable the study of the mode of action of cytotoxic agents in their intended environment.

### 5.2. Cellular navigation and phagocytosis

The respiratory tract is continually exposed to non-sterile air. This evokes the question as to how the lower respiratory tract deals with inhaled pathogens. Most pathogens will be cleared by the upper respiratory tract, though bacteria that manage to pass through, still bear the potential to infect alveoli in the lower tract [130]. For the better part of research, alveolar macrophages have been thought of as sessile, non-motile immune agents [131–133] and due to being outnumbered by the sum of all alveoli [134], were not considered as the primary means of innate defense responsible for the lower respiratory tract. However, an alternative explanation provided by the engagement of neutrophils would imply a state of constant respiratory inflammation, which is far from what is being observed.

Research employing multichannel spinning-disk intravital microscopy through an intercostal lung window in mice gives credence to the hypothesis of motile alveolar macrophages [135].

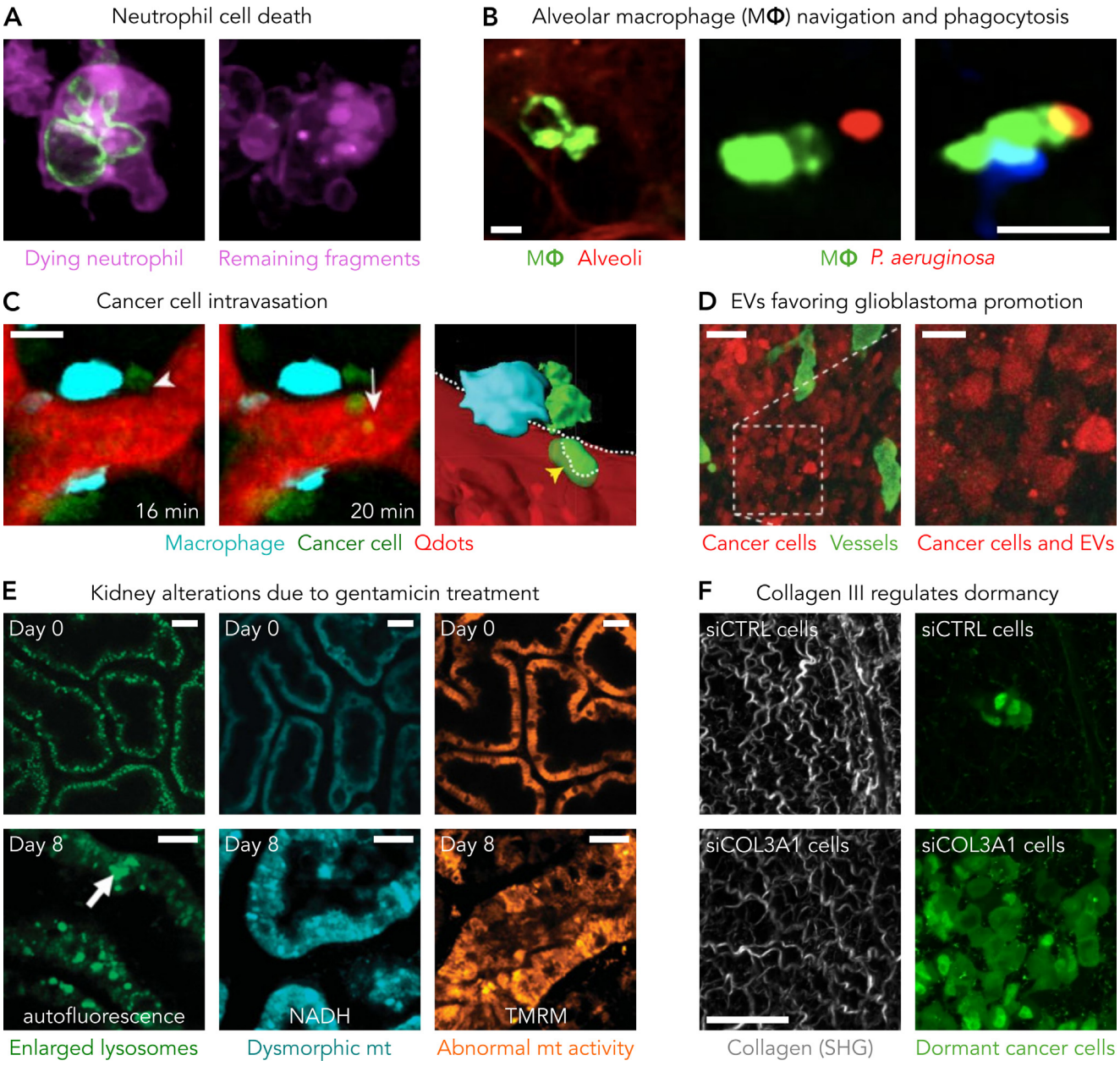


**Fig. 8. Visualizing dynamic biological processes with IVM. (A)** Intravital LLSM of a dying neutrophil with a hypersegmented nucleus and its subsequent clearing by neighboring neutrophils. While the nucleus is entirely cleared, only fragments remain. **(B)** Visualization of PKH26 labelled alveolar macrophages migrating from one alveolus to a neighboring one and migrating towards and phagocytosing pathogenic P. aeruginosa. **(C)** IVM time-lapse of a tumor cell performing transendothelial migration at the tumor microenvironment of metastasis and a 3D reconstruction of the intravasation process. **(D)** MP-IVM of a glioblastoma trough an implanted brain window in mice shows fluorescent punctae resembling extracellular vesicles and their colocalization with glioma cells. **(E)** Intravital imaging of the kidney shows the intracellular changes occurring after administration of gentamicin. Changes in the green autofluorescence suggest enlargement of lysosomes, while changes in morphology and intensity of NADPH autofluorescence are evidence for dysfunctional and dysmorphic mitochondria, which is corroborated by changes in the TMRM signals. **(F)** MP-IVM of mice intravenously injected with COL3A1 silenced dormant D-Hep3 cells indicates a significant increase in proliferation and metastasis as compared to mice injected with control D-Hep3 cells. All images were adapted with permission [83,135,143,147,156,157]. (For interpretation of the references to color in this figure legend, the reader is referred to the web version of this article.)

Here, the authors have not only revealed the ability of alveolar macrophages to migrate between alveoli through the pores of Kohn, but have further demonstrated their ability to chemotax towards and phagocytose pathogenic bacteria (Fig. 8**B**). Apart from increasing our understanding of alveolar macrophages, this application of IVM has demonstrably affirmed its potential to settle questions on the dynamics of otherwise experimentally inaccessible processes. The study of host-pathogen interactions has not been limited to the respiratory setting, however. The impact of IVM on the imaging of such interactions as they occur in the brain has been captured elsewhere [136].

### *5.3. Tumor cell intravasation*

The mechanisms behind cancer cell motility and cell state plasticity, although essential to the understanding of metastasis and tumor cell invasion, are still largely unknown. Both processes are influential in the anticancer drug response, and comprehension of these processes could lead to the discovery of new druggable targets or therapeutic strategies for the treatment of metastasis. The discovery of these processes surrounding metastasis has benefited greatly from the ability of IVM to track and visualize migrating tumor cells over time at cellular resolution (the impact of IVM

on cell motility and cell state plasticity has been reviewed elsewhere [137,138]).

The significance of perivascular macrophages in the tumor microenvironment of metastasis (TMEM) as well as their implication in tumor cell intravasation has been widely described throughout the literature [18,139–142]. However, beyond their functional association, nothing substantial was previously known about the mechanism of interaction. In a study employing high-resolution MP-IVM the aforementioned interaction as well as tumor cell intravasation was more closely visualized [143]. Not only was it discovered that incidences of intravasation of motile tumor cells occur at the TMEM but further that transient local blood vessel permeability mostly occurred in combination with these intravasation events (Fig. 8**C**).

### 5.4. Tumor promotion via extracellular vesicles

It has been long postulated that oncogenic extracellular vesicles serve as the mediator of brain malignancies to subvert their microenvironment towards the promotion of carcinogenic and metastatic phenotypes [144]. Glioblastomas, albeit only rarely metastasizing, exploit this mechanism to promote their own tumor growth [144]. There is growing evidence that glioblastomas, among other means, transfer instructional, extracellular RNA via extracellular vesicles to recipient cells in the TME [145,146], amongst which microglia play a significant role.

IVM in a syngeneic GL261 murine glioma model [147] was used to investigate, *in situ*, the internalization of glioma-derived extracellular vesicles by microglia and macrophages. GL261 tumors, manipulated to release fluorescent extracellular vesicles (red), in C57BL/6 CX3CR1$^{GFP+}$ mice producing GFP-expressing microglia and macrophages, were imaged by MP-IVM via a cortical brain window (Fig. 8**D**). Red fluorescent dots and other structures encompassing the tumor cells were observed, resemblant in morphology of extracellular vesicles. The presumed extracellular vesicles were of relatively large size ranging from above- to somewhat sub-micrometer dimensions. The inability of the imaging system to visualize smaller extracellular vesicles imparts the assumption that the detected extracellular vesicles may only constitute to a fraction of existent extracellular vesicles. Nonetheless, the principal findings demonstrate the co-localization of extracellular vesicles with microglia and macrophages, either on the cell surface or intracellularly. This serves as evidence for the *in vivo* internalization of extracellular vesicles by recipient cells such as microglia in the glioma-bearing brain using IVM.

### 5.5. Structural and functional tissue alterations

Cell death provides an essential function to many tissues [148]. In the renal tissue, the dysregulation of CD plays an important role in the etiology of major renal diseases [149,150], commonly escalating into life threatening conditions in patients [151] (NB: techniques of IVM applicable to the study of renal cell death dynamics are already extensively reviewed [122]). Over the course of two decades [152,153], MP-IVM has substantiated itself as the gold standard technique [154] to produce not only informative images of renal systems, but moreover helps to elucidate the dynamic physiology of the kidney from a tissue to a subcellular scale.

MP-IVM was applied in Munich Wistar Frömter rats to visualize glomerular filtration after a bolus injection of lucifer yellow. The filtration of lucifer yellow into the Bowman's space and its subsequent accumulation in the proximal tubule was observed. Furthermore, the visualization of necrotic cell death (using propidium iodide) of the glomerular vasculature in response to laser-induced damage in the rats, illustrates how cells in the glomerulus undergo a necrotic pathway following photo laser injury, as indicated by the nuclei PI staining of cells adjacent to the site of injury. Intravital imaging has been shown to resolve select fundamental renal structures in rats, such as the distal tubule (DT) and glomerulus (G), while also distinguishing the two substructures of proximal tubules, namely S1 and S2. Imaging of the plasma streaming through the peritubular capillaries of the renal cortex in mice, illustrates its application in the study of renal capillary blood flow using line scanning. Reactive oxygen species (ROS), a common by-product of mitochondrial metabolism, play a significant role in specific pathways of regulated cell death. Ischemia-reperfusion injury in the kidney can cause a peak in ROS generation, however, whether the peak occurred during ischemia or subsequent reperfusion remained unknown [155]. MPM of ROS generation in the proximal tubules upon ischemia–reperfusion injury, visualized using the superoxide-sensitive dye dihydroethidium, demonstrated a steady peak of ROS generation throughout the duration of ischemia well into the process of reperfusion (Fig. 8**E**). In this experimental setup, dihydroethidium, in the presence of superoxides, dehydrates and subsequently localizes to the nucleus, where it can be detected via its fluorescence [156].

### 5.6. The influence of extracellular matrix on tumor dormancy

The extracellular matrix is a conglomerate of different proteins, arranging structural support for tumors while further engaging in the modulation of tumor metastasis. The structure of the ECM, in particular of collagen, itself has been shown to correlate with poor prognosis of i.e., breast cancer patients. Revealing how collagen structure correlates with for example metastasis and tumor dormancy, may provide greater insight on these mechanisms as well as present novel approaches on the intervention of these malignancies.

Using SHG of collagen in intravital multiphoton microscopy, it was revealed that tumor cells contribute to and localize with pro-dormant ECM niches and further confirmed the plasticity of said niches [157]. Intravital imaging in immunocompetent as well as immunodeficient mice further identified that the dormancy of tumor growth can be triggered by the enrichment of collagen type III (Fig. 8**F**).

## 6. Outlook

The range in scale and resolution made available by intravital microscopy is certainly powerful. Nonetheless, many of the profound discoveries were achieved when IVM was not used as a standalone tool, but rather when combined with techniques such as whole-body imaging and flow cytometry. Indeed, studies tackling the clinical success of nanomedicines will certainly get closer to the bigger picture through a multimodal and multiscale approach to, for example, reveal the spatially heterogeneous distribution of nanomedicines. Flow cytometry, on the other hand, will further elaborate on the cellular populations and subpopulations involved in the processes observed using IVM and in the process reveal the intricate interactions and involvements of e.g., immune cells in drug delivery and release. Similarly, increasingly smaller and more capable multimodal reporters will further bridge the gap between IVM and whole-body imaging [158,159].

The ability to dynamically visualize therapeutic and diagnostic procedures makes intravital microscopy a strong asset in the assessment and development of (nano)therapies, diagnostic imaging probes, and theranostic agents. In the current perspective, this asset will gain further potential when accompanied by functional reporters. Especially the advent of multiplex labelling of window chambered tumor models [160], which is akin to *in vivo* flow

cytometry, may open up further opportunities, especially for the study of the TME and other complex cellular milieus. This method utilizes a scission-accelerated fluorophore exchange (SAFE) to entirely remove a fluorophore from previously labeled cells within dorsal and cranial window chambers in mice. This allows for the ability to perform cyclic imaging of specific cell types *in vivo*, as was demonstrated via 12 color imaging of immune cells in live mice.

While IVM directly benefits from advances made in fields such as microscopy, it is equally exposed to their pitfalls. The pronounced caveats of IVM are (1) its limited tissue penetration, (2) as well as the required interventional preparation of the subjects of study, (3) the difficulty of using fluorescent probes in tissues with high influx and efflux of liquids and interfering metabolites (such as the kidneys), (4) the lack of direct fluorescence intensity based quantification over time, (5) and the challenge of monitoring chronic events in the same mouse over an extended period of time. While the limits of penetration depth are challenged through the application of i.e., three-photon microscopy and improvements in surgical methodologies, they still remain distinct limits of IVM. In the meantime, combining IVM with other *in vivo* (whole body) imaging modalities may showcase an alleviation of said shortcomings.

Currently, the majority of studies using IVM provide mostly observational as opposed to experimental information. To drive the utility of IVM forward, it is essential to steer IVM into a more interrogatory direction. For instance, through the development and use of IVM-suitable probes (e.g., FRET-biosensors), molecular processes such as intra- and intercellular signaling and the development of chemotherapeutic resistance are topics on the horizon. Likewise, additional mice and tumor models are needed that reflect the aforementioned approach [161–163]. This goes hand-in-hand with the prospect of translational IVM. The majority of current tumor models used in IVM neither reflect the natural oncogenesis nor the morphology and microenvironment of human tumors in the clinic. Correspondingly, in order to facilitate the transition towards more translatable IVM, preclinical models for IVM have to become clinically more relevant. In that regard, IVM in the clinic will certainly find its niche in the non-invasive and diagnostic imaging of cancerous lesions and may find significant use as an intraoperative guide for targeted biopsies and therapy prognosis.

Generally, IVM has proven essential in the discovery of many *in vivo* processes and mechanisms in the past, as has been highlighted in the previous chapters, and its utility may expand with an ever-growing arsenal of tools and techniques. In the following sections, the efforts and hurdles of clinical translation regarding IVM, as well as the advantages of machine learning as applied to intravital imaging will be put into perspective.

### 6.1. Clinical translation

Intravital microscopy enables the preclinical study of both quantitative and qualitative aspects of biology or biomedicine with excellent proficiency. Given this premise, there is a clear incentive for its translation into the clinic. There, it is anticipated to provide a detailed analysis of individual patients, consequently laying ground for personalized medicine and informing about therapeutic outcome [164,165]. However, this premise does not take into account that, unlike whole body imaging, many observations in IVM necessitate surgical intervention and in many preclinical set ups even exteriorized tissue and organs. The invasive nature of a significant portion of IVM procedures is usually not offset by its benefits, in a clinical setting. With improving technology and therefore financial and procedural convenience, however, we are beginning to see a shift towards the intraoperative application of IVM. In a recent pilot trial, intraoperative and intravital (probe based) confocal laser endomicroscopy was used to study the tumor vasculature of peritoneal carcinomatosis (PC) patients [166]. As aberrancies in the tumor microvasculature are known to interfere with drug delivery of chemotherapeutics, it was proposed that during cytoreductive surgery and preceding hyperthermic intraperitoneal chemotherapy, IVM could be performed on the patient. The hypothesis stated that by directly acquiring vessel characteristics using IVM, a potential link between these vessel properties and oncological outcome could be drawn. However, the outcome of the study did not confirm said hypothesis, as no such link could be identified in the scope of this pilot trial, despite successful IVM on all patients. Nonetheless, larger clinical trials are currently aiming to determine the clinical use of IVM in PC and solid tumor patients (NCT03517852 and NCT03823144) [167,168].

Currently, the majority of translational IVM comes in the form of fiber-optic, probe-based endoscopy (mostly confocal laser-scanning endoscopy). This circumvents many of the invasive issues tied to IVM but also greatly reduces the pool of application [2]. Also sidestepping the need for invasive procedures, there are commercially available intravital multiphoton FLIM (IV-MP-FLIM) setups, which are intended for use in the clinical setting. There have been multiple recent reports claiming clinically translatable methods that apply IV-MP-FLIM, though mostly on malignancies of the skin and other external cancerous lesions [169–173]. These efforts may represent early attempts; hence, success or mere feasibility have not been demonstrated yet. Even in the event of verified feasibility, translation to the clinic will pose other significant challenges along the way, leaving it as a topic for the still distant future.

### 6.2. Potential impact of artificial intelligence

With the steady increase of improvements made to IVM comes an upsurge in the size of data and the complexity of its acquisition. This, in turn, raises the complexity of and therefore time spend in post-imaging data processing and analysis. Especially with the rise of quantitative IVM analyses and the added potential for more detailed statistical investigation and reduced personal bias through less user dependence, does machine learning lend itself as a viable solution. Deep learning, as a class of machine learning, comprises a group of algorithms equipped to compile raw data inputs into a network of multiple layers from which a greater level of features are derived from. IVM, as a data-rich field, inherently faces the challenge of complex and at times ill-understood and misleading results. Hence, the application of machine learning, especially deep learning, presents itself as an increasingly fitting technique to combat said challenge. Though, despite these confident claims and the impressive impact of deep learning in medical research as a whole [174], deep learning is comparatively speaking still in its infancy as applied to intravital microscopy. Nonetheless, the use of e.g., correction tools for tissue movement and similar tasks can currently be partially automated, reducing operator and confirmation biases. Furthermore, the generation of multidimensional imaging data is alleviated through the use of such automation algorithms. Likewise, the extended examination of increasingly prevalent quantitative data in IVM may uncover patterns previously hidden by convolution and complexity of the data.

As an example, cell cycle deregulation has been shown to contribute to a host of diseases. It is especially recognized as one of the hallmarks of cancer and its study has gained an increase in interest accordingly. Traditionally, our knowledge of cell cycle regulation and progression stems from 2D and *ex vivo* experimentation. However, IVM has caught notice as a means to study these systems under precise physiological conditions. Though the current best practice is the manual annotation and analysis of arbitrarily sampled data. The following proof-of-concept study has profiled cell cycle progression in xenograft

tumors using quantitative IVM [175]. An integrated workflow is shown in which cell cycle effects of several antimitotic cancer drugs in HT1080 fibrosarcoma xenografts were quantified and compared in living mice over the duration of 8 days. The results demonstrate that not only the quantity but further the quality of data can be significantly increased via deep learning assisted data acquisition and analysis. Especially the scoring of numerous single events enables researchers to better put such data into the correct biological context and significantly decreases time spent on data analysis.

Moreover, the morphology in size and shape as well as behavior are properties of immune cells that vary greatly from one organ to another and even from session to session in intravital microscopy. Unlike in live cell imaging, here, cells of interest are intertwined with the heterogeneous background of unpredictable patterns. As in the previous example, manual counting and interpretation is still the most widespread technique. In a study, a convolutional neural network was developed, leaning on an existing single stage object detection network called RetinaNet, to automate and standardize leukocyte detection and further their recruitment for IVM. This immunoinformatic tool generated results absent of overfitting and proved invariant to the variability of cells [176]. In order to facilitate longitudinal tracking of cell populations, these populations first require segmentation from the background. A group of multicolored cancer cell lines have been generated to provide reliable segmentation capabilities using automated, hue selection based algorithms [177]. The application of these or similar machine learning algorithms are scarce as of yet. Nonetheless, semiautomated machine learning analysis on segmented migrating tumor cells was utilized in a study on the link between the TME and tumor cell phenotype [178]. The predictive power of these analytic methods was demonstrated by their ability to classify heterogeneous TMEs and consequently correlate tumor cell behavior with localization.

Despite the apparent suitability and clear demand, AI and machine learning in particular are still emerging tools utilized only scarcely within the field of intravital microscopy. In the overarching fields that influence intravital microscopy, such as microscopy, biology and biomedicine, these algorithms are gaining ground in both application as well as technology (as comprehensively reviewed elsewhere [174,179–181]). In light of growing demand, rising availability and ease-of-use, it is expected for machine learning to have a much greater impact in the near future.

## 7. Conclusions

As amply exemplified in the preceding sections, IVM has enabled the exploration of numerous processes in their native environment. Importantly, considering its high spatiotemporal resolution (i.e., real-time dynamic information at the tissue and cellular level), it has served as a link between whole-body imaging techniques (e.g., PET, MRI), and fundamental ex vivo analytical techniques at the cell level (e.g., flow cytometry). Due to this, it has substantially improved our possibilities to uncover novel processes, as for example was demonstrated in the discovery of nanoparticle active targeting mechanisms, immune cell behavior, and cellular organization [182]. These notable developments declare an upsurge of exciting new discoveries yet to come. Nonetheless, while some effort is made towards a meaningful translation of IVM to the clinic, as of yet, no significant milestones have been achieved. With regard to data acquisition and processing, the increasing magnitude of data produced is currently being countered by the development of machine learning and in particular deep learning algorithms that allow for fast and less biased screening and quantification.

Taken together, IVM has been and will continue to be instrumental in the discovery and clarification of structure and function of living systems. For this reason, the integration of IVM into a multimodal network of tools (i.e., combined with flow cytometry, whole-body imaging, etc.) will considerably boost its utility in drug delivery and bioengineering applications.

## Data availability

No data was used for the research described in the article.

## Declaration of Competing Interest

The authors declare that they have no known competing financial interests or personal relationships that could have appeared to influence the work reported in this paper.

## Acknowledgements

The authors gratefully acknowledge financial support by the European Fund for Regional Development (TL – TAKTIRA: Project number: EFRE-0801767)), the European Research Council (TL – ERC Consolidator Grant 864121: Meta-Targeting), the German Research Foundation (TL – DFG: GRK2375 (Project number: 331065168); AMS – DFG RWTH JPI Excellence Initiative; TL, AMS – CRC1066 grant for project B17), the German Federal Ministry of Research and Education (TL – BMBF: PP-TNBC, Project number 16GW0319K), and the German Cancer Aid (AMS – SDK Postgraduate Program MSSO$^{ABCD}$).

## References

[1] M.J. Pittet, R. Weissleder, Intravital imaging, Cell 147 (2011) 983–991, https://doi.org/10.1016/J.CELL.2011.11.004.
[2] K. Van Dyck, E. Vanhoffelen, J. Yserbyt, P. Van Dijck, M. Erreni, S. Hernot, G., Vande Velde, Probe-based intravital microscopy: filling the gap between in vivo imaging and tissue sample microscopy in basic research and clinical applications, J. Phys. Photon. 3 (2021) 032003, https://doi.org/10.1088/2515-7647/AC0804.
[3] F. Lassailly, K. Foster, L. Lopez-Onieva, E. Currie, D. Bonnet, Multimodal imaging reveals structural and functional heterogeneity in different bone marrow compartments: functional implications on hematopoietic stem cells, Blood 122 (2013) 1730–1740, https://doi.org/10.1182/BLOOD-2012-11-467498.
[4] T. Hara, B. Bhayana, B. Thompson, C.W. Kessinger, A. Khatri, J.R. McCarthy, R. Weissleder, C.P. Lin, G.J. Tearney, F.A. Jaffer, Molecular imaging of fibrin deposition in deep vein thrombosis using a new fibrin-targeted near-infrared fluorescence (NIRF) imaging strategy, JACC. Cardiovasc. Imag. 5 (2012) 607, https://doi.org/10.1016/J.JCMG.2012.01.017.
[5] M.A. Karreman, L. Mercier, N.L. Schieber, G. Solecki, G. Allio, F. Winkler, B. Ruthensteiner, J.G. Goetz, Y. Schwab, Fast and precise targeting of single tumor cells in vivo by multimodal correlative microscopy, J. Cell Sci. 129 (2016) 444, https://doi.org/10.1242/JCS.181842.
[6] A.M. Sofias, F. De Lorenzi, Q. Peña, A. Azadkhah Shalmani, M. Vucur, J.W. Wang, F. Kiessling, Y. Shi, L. Consolino, G. Storm, T. Lammers, Therapeutic and diagnostic targeting of fibrosis in metabolic, proliferative and viral disorders, Adv. Drug Deliv. Rev. 175 (2021) 113831, https://doi.org/10.1016/J.ADDR.2021.113831.
[7] J.S. de Maar, A.M. Sofias, T.P. Siegel, R.J. Vreeken, C. Moonen, C. Bos, R. Deckers, Spatial heterogeneity of nanomedicine investigated by multiscale imaging of the drug, the nanoparticle and the tumour environment, Theranostics 10 (2020) 1884, https://doi.org/10.7150/THNO.38625.
[8] M. Rytelewski, K. Haryutyunan, F. Nwajei, M. Shanmugasundaram, P. Wspanialy, M.A. Zal, C.H. Chen, M. El Khatib, S. Plunkett, S.A. Vinogradov, M. Konopleva, T. Zal, Merger of dynamic two-photon and phosphorescence lifetime microscopy reveals dependence of lymphocyte motility on oxygen in solid and hematological tumors, J. Immunother. Cancer. 7 (2019) 78, https://doi.org/10.1186/S40425-019-0543-Y.
[9] M. Desjardins, K. Kılıç, M. Thunemann, C. Mateo, D. Holland, C.G.L. Ferri, J.A. Cremonesi, B. Li, Q. Cheng, K.L. Weldy, P.A. Saisan, D. Kleinfeld, T. Komiyama, T.T. Liu, R. Bussell, E.C. Wong, M. Scadeng, A.K. Dunn, D.A. Boas, S. Sakadžić, J. B. Mandeville, R.B. Buxton, A.M. Dale, A. Devor, Awake mouse imaging: from two-photon microscopy to blood oxygen level-dependent functional magnetic resonance imaging, Biol. Psychiatry Cogn. Neurosci. Neuroimag. 4 (2019) 533–542, https://doi.org/10.1016/J.BPSC.2018.12.002.

[10] C.D. Schuh, D. Haenni, E. Craigie, U. Ziegler, B. Weber, O. Devuyst, A.M. Hall, Long wavelength multiphoton excitation is advantageous for intravital kidney imaging, Kidney Int. 89 (2016) 712–719, https://doi.org/10.1038/KI.2015.323/ATTACHMENT/20B9AF66-66E6-46F2-B9E8-DED573595625/MMC2.MP4.
[11] N.G. Horton, K. Wang, D. Kobat, C.G. Clark, F.W. Wise, C.B. Schaffer, C. Xu, In vivo three-photon microscopy of subcortical structures within an intact mouse brain, Nat. Photon. 73. 7 (2013) 205–209. <https://doi.org/10.1038/nphoton.2012.336>.
[12] V. Andresen, S. Alexander, W.M. Heupel, M. Hirschberg, R.M. Hoffman, P. Friedl, Infrared multiphoton microscopy: subcellular-resolved deep tissue imaging, Curr. Opin. Biotechnol. 20 (2009) 54–62, https://doi.org/10.1016/J.COPBIO.2009.02.008.
[13] D. Kedrin, B. Gligorijevic, J. Wyckoff, V. V. Verkhusha, J. Condeelis, J.E. Segall, J. van Rheenen, Intravital imaging of metastatic behavior through a mammary imaging window, Nat. Methods 2008 512. 5 (2008) 1019–1021. <https://doi.org/10.1038/nmeth.1269>.
[14] M. Egeblad, A.J. Ewald, H.A. Askautrud, M.L. Truitt, B.E. Welm, E. Bainbridge, G. Peeters, M.F. Krummel, Z. Werb, Visualizing stromal cell dynamics in different tumor microenvironments by spinning disk confocal microscopy, Dis. Model. Mech. 1 (2008) 155–167, https://doi.org/10.1242/DMM.000596.
[15] A.D. Bins, J. van Rheenen, K. Jalink, J.R. Halstead, N. Divecha, D.M. Spencer, J.B. Haanen, T.N.M. Schumacher, Intravital imaging of fluorescent markers and FRET probes by DNA tattooing, BMC Biotechnol. 7 (2007) 1–7, https://doi.org/10.1186/1472-6750-7-2/FIGURES/5.
[16] B. Breart, F. Lemaître, S. Celli, P. Bousso, Two-photon imaging of intratumoral CD8+ T cell cytotoxic activity during adoptive T cell therapy in mice, J. Clin. Invest. 118 (2008) 1390–1397, https://doi.org/10.1172/JCI34388.
[17] M. Bajénoff, J.G. Egen, L.Y. Koo, J.P. Laugier, F. Brau, N. Glaichenhaus, R.N. Germain, Stromal cell networks regulate lymphocyte entry, migration, and territoriality in lymph nodes, Immunity 25 (2006) 989–1001, https://doi.org/10.1016/J.IMMUNI.2006.10.011/ATTACHMENT/2602B260-1FBA-47ED-B063-C170886C7396/MMC14.AVI.
[18] J.B. Wyckoff, Y. Wang, E.Y. Lin, J.F. Li, S. Goswami, E.R. Stanley, J.E. Segall, J.W. Pollard, J. Condeelis, Direct visualization of macrophage-assisted tumor cell intravasation in mammary tumors, Cancer Res. 67 (2007) 2649–2656, https://doi.org/10.1158/0008-5472.CAN-06-1823.
[19] J. Livet, T.A. Weissman, H. Kang, R.W. Draft, J. Lu, R.A. Bennis, J.R. Sanes, J.W. Lichtman, Transgenic strategies for combinatorial expression of fluorescent proteins in the nervous system, Nat. 4507166 (450) (2007) 56–62, https://doi.org/10.1038/nature06293.
[20] M. Rueckel, J.A. Mack-Bucher, W. Denk, Adaptive wavefront correction in two-photon microscopy using coherence-gated wavefront sensing, Proc. Natl. Acad. Sci. U. S. A. 103 (2006) 17137–17142, https://doi.org/10.1073/PNAS.0604791103/ASSET/85C6E3B5-6750-4BAF-B2E2-1A8AA0172180/ASSETS/GRAPHIC/ZPQ04606-4109-M02.JPEG.
[21] G. Dong, N. Ray, S.T. Acton, Intravital leukocyte detection using the gradient inverse coefficient of variation, IEEE Trans. Med. Imaging. 24 (2005) 910–924, https://doi.org/10.1109/TMI.2005.846856.
[22] T.R. Mempel, M.L. Scimone, J.R. Mora, U.H. Von Andrian, In vivo imaging of leukocyte trafficking in blood vessels and tissues, Curr. Opin. Immunol. 16 (2004) 406–417, https://doi.org/10.1016/J.COI.2004.05.018.
[23] E. Brown, T. McKee, E. DiTomaso, A. Pluen, B. Seed, Y. Boucher, R.K. Jain, Dynamic imaging of collagen and its modulation in tumors in vivo using second-harmonic generation, Nat. Med. 96 (9) (2003) 796–800, https://doi.org/10.1038/nm879.
[24] M. Seshadri, J.A. Spernyak, P.G. Maier, R.T. Cheney, R. Mazurchuk, D.A. Bellnier, Visualizing the acute effects of vascular-targeted therapy in vivo using intravital microscopy and magnetic resonance imaging: correlation with endothelial apoptosis, cytokine induction, and treatment outcome, Neoplasia. 9 (2007) 128–135, https://doi.org/10.1593/NEO.06748.
[25] M. Neeman, H. Dafni, O. Bukhari, R.D. Braun, M.W. Dewhirst, In vivo BOLD contrast MRI mapping of subcutaneous vascular function and maturation: Validation by intravital microscopy, Magn. Reson. Med. 45 (2001) 887–898, https://doi.org/10.1002/MRM.1118.
[26] M.J. Miller, S.H. Wei, I. Parker, M.D. Cahalan, Two-photon imaging of lymphocyte motility and antigen response in intact lymph node, Science 296 (2002) 1869–1873, https://doi.org/10.1126/SCIENCE.1070051.
[27] E.B. Brown, R.B. Campbell, Y. Tsuzuki, L. Xu, P. Carmeliet, D. Fukumura, R.K. Jain, In vivo measurement of gene expression, angiogenesis and physiological function in tumors using multiphoton laser scanning microscopy, Nat. Med. 77 (7) (2001) 864–868, https://doi.org/10.1038/89997.
[28] K. Svoboda, W. Denk, D. Kleinfeld, D.W. Tank, In vivo dendritic calcium dynamics in neocortical pyramidal neurons, Nature 3856612 (385) (1997) 161–165, https://doi.org/10.1038/385161a0.
[29] G.N. Naumov, S.M. Wilson, I.C. MacDonald, E.E. Schmidt, V.L. Morris, A.C. Groom, R.M. Hoffman, A.F. Chambers, Cellular expression of green fluorescent protein, coupled with high-resolution in vivo videomicroscopy, to monitor steps in tumor metastasis, J. Cell Sci. 112 (1999) 1835–1842, https://doi.org/10.1242/JCS.112.12.1835.
[30] K.L. Farina, J.B. Wyckoff, J. Rivera, H. Lee, J.E. Segall, J.S. Condeelis, J.G. Jones, J. S. Câ, and Pathologv Â, J.G. JJ Albert, Cell Motility of Tumor Cells Visualized in Living Intact Primary Tumors Using Green Fluorescent Protein1, CANCER Res. 5 (1998) 2528–2532. <http://aacrjournals.org/cancerres/article-pdf/58/12/2528/2861788/cr0580122528.pdf> (Accessed August 8, 2022).
[31] J.G. White, W.B. Amos, M. Fordham, An evaluation of confocal versus conventional imaging of biological structures by fluorescence light microscopy, J. Cell Biol. 105 (1987) 41–48, https://doi.org/10.1083/JCB.105.1.41.
[32] G.J. Brakenhoff, H.T.M. van der Voort, E.A. van Spronsen, N. Nanninga, Three-dimensional imaging in fluorescence by confocal scanning microscopy, J. Microsc. 153 (1989) 151–159, https://doi.org/10.1111/J.1365-2818.1989.TB00555.X.
[33] W. Denk, J.H. Strickler, W.W. Webb, Two-photon laser scanning fluorescence microscopy, Science (80-.). 248 (1990) 73–76. <https://doi.org/10.1126/SCIENCE.2321027>.
[34] E.E. Hoover, J.A. Squier, Advances in multiphoton microscopy technology, Nat. Photon. 72 (7) (2013) 93–101, https://doi.org/10.1038/nphoton.2012.361.
[35] C. Xu, W. Zipfel, J.B. Shear, R.M. Williams, W.W. Webb, Multiphoton fluorescence excitation: new spectral windows for biological nonlinear microscopy, Proc. Natl. Acad. Sci. 93 (1996) 10763–10768, https://doi.org/10.1073/PNAS.93.20.10763.
[36] H. SW, B. K, S. M, S. A, M. HM, G. I, L. JR, Three-photon excitation in fluorescence microscopy, J. Biomed. Opt. 1 (1996) 71. <https://doi.org/10.1117/12.229062>.
[37] X. Liu, B. Li, X. Li, A.R. Harutyunyan, J. Hone, D.V. Esposito, The critical role of electrolyte gating on the hydrogen evolution performance of monolayer MoS2, Nano Lett. 19 (2019) 8118–8124, https://doi.org/10.1021/ACS.NANOLETT.9B03337/SUPPL_FILE/NL9B03337_SI_001.PDF.
[38] W. Becker, Fluorescence lifetime imaging – techniques and applications, J. Microsc. 247 (2012) 119–136, https://doi.org/10.1111/J.1365-2818.2012.03618.X.
[39] R.M. Power, J. Huisken, A guide to light-sheet fluorescence microscopy for multiscale imaging, Nat. Methods 144 (14) (2017) 360–373, https://doi.org/10.1038/nmeth.4224.
[40] J. Huisken, J. Swoger, F. Del Bene, J. Wittbrodt, E.H.K. Stelzer, Optical sectioning deep inside live embryos by selective plane illumination microscopy, Science (80-.). 305 (2004) 1007–1009. <https://doi.org/10.1126/SCIENCE.1100035/SUPPL_FILE/HUISKEN.SOM.PDF>.
[41] P.-Y. Lin, S.-P.L. Hwang, C.-H. Lee, B.-C. Chen, Two-photon scanned light sheet fluorescence microscopy with axicon imaging for fast volumetric imaging, Https://Doi.Org/10.1117/1.JBO.26.11.116503. 26 (2021) 116503. <https://doi.org/10.1117/1.JBO.26.11.116503>.
[42] V. Andresen, K. Pollok, J.L. Rinnenthal, L. Oehme, R. Günther, H. Spiecker, H. Radbruch, J. Gerhard, A. Sporbert, Z. Cseresnyes, A.E. Hauser, R. Niesner, High-Resolution Intravital Microscopy, PLoS One. 7 (2012) e50915.
[43] H. Steffens, W. Wegner, K.I. Willig, In vivo STED microscopy: a roadmap to nanoscale imaging in the living mouse, Methods. 174 (2020) 42–48, https://doi.org/10.1016/J.YMETH.2019.05.020.
[44] D. Soulet, J. Lamontagne-Proulx, B. Aubé, D. Davalos, Multiphoton intravital microscopy in small animals: motion artefact challenges and technical solutions, J. Microsc. 278 (2020) 3–17, https://doi.org/10.1111/JMI.12880.
[45] A. Masedunskas, O. Milberg, N. Porat-Shliom, M. Sramkova, T. Wigand, P. Amornphimoltham, R. Weigert, Intravital microscopy: a practical guide on imaging intracellular structures in live animals, Bioarchitecture. 2 (2012) 143–157, https://doi.org/10.4161/BIOA.21758/SUPPL_FILE/KBIA_A_10921758_SM0001.ZIP.
[46] C. Prunier, N. Chen, L. Ritsma, N. Vrisekoop, Procedures and applications of long-term intravital microscopy, Methods. 128 (2017) 52–64, https://doi.org/10.1016/J.YMETH.2017.06.029.
[47] M.A. Karreman, V. Hyenne, Y. Schwab, J.G. Goetz, Intravital correlative microscopy: imaging life at the nanoscale, Trends Cell Biol. 26 (2016) 848–863, https://doi.org/10.1016/J.TCB.2016.07.003.
[48] M. Hao, K. Flynn, C. Nien-Shy, B.E. Jester, M. Winkler, D.J. Brown, O. La Schiazza, J. Bille, J.V. Jester, In vivo non-linear optical (NLO) imaging in live rabbit eyes using the Heidelberg Two-Photon Laser Ophthalmoscope, Exp. Eye Res. 91 (2010) 308–314, https://doi.org/10.1016/J.EXER.2010.06.007.
[49] C. Schwarz, R. Sharma, W.S. Fischer, M. Chung, G. Palczewska, K. Palczewski, D.R. Williams, J.J. Hunter, K. Tsunoda, G. Hanazono, K. Inomata, Y. Kazato, W. Suzuki, M. Tanifuji, Safety assessment in macaques of light exposures for functional two-photon ophthalmoscopy in humans, Biomed. Opt. Express 7 (12) (2016) 5148–5169. <https://doi.org/10.1364/BOE.7.005148>.
[50] A. Batista, H.G. Breunig, T. Hager, B. Seitz, K. König, Early evaluation of corneal collagen crosslinking in ex-vivo human corneas using two-photon imaging, Sci. Reports 2019 91. 9 (2019) 1–9. <https://doi.org/10.1038/s41598-019-46572-3>.
[51] E. Dondossola, P. Friedl, Host responses to implants revealed by intravital microscopy, Nat. Rev. Mater. 71 (7) (2021) 6–22, https://doi.org/10.1038/s41578-021-00369-x.
[52] C. Wang, C. Xia, Y. Zhu, H. Zhang, Innovative fluorescent probes for in vivo visualization of biomolecules in living Caenorhabditis elegans, Cytom. Part A 99 (2021) 560–574, https://doi.org/10.1002/CYTO.A.24325.
[53] E. Rebollo, K. Karkali, F. Mangione, E. Martín-Blanco, Live imaging in Drosophila: the optical and genetic toolkits, Methods. 68 (2014) 48–59, https://doi.org/10.1016/J.YMETH.2014.04.021.
[54] S. Dunst, P. Tomancak, Imaging Flies by fluorescence microscopy: principles, technologies, and applications, Genetics. 211 (2019) 15, https://doi.org/10.1534/GENETICS.118.300227.
[55] S. Sieber, P. Grossen, J. Bussmann, F. Campbell, A. Kros, D. Witzigmann, J. Huwyler, Zebrafish as a preclinical in vivo screening model for

nanomedicines, Adv. Drug Deliv. Rev. 151–152 (2019) 152–168, https://doi.org/10.1016/J.ADDR.2019.01.001.
[56] I.J. Marques, E. Lupi, N. Mercader, Model systems for regeneration: Zebrafish, Dev. 146 (2019), https://doi.org/10.1242/DEV.167692/224198.
[57] P. Pantazis, W. Supatto, Advances in whole-embryo imaging: a quantitative transition is underway, Nat. Rev. Mol. Cell Biol. 155 (15) (2014) 327–339, https://doi.org/10.1038/nrm3786.
[58] A. Coste, M.H. Oktay, J.S. Condeelis, D. Entenberg, Intravital imaging techniques for biomedical and clinical research, Cytom. Part A 97 (2020) 448–457, https://doi.org/10.1002/CYTO.A.23963.
[59] A.M. Sofias, A.K.O. Åslund, N. Hagen, K. Grendstad, S. Hak, Simple and robust intravital microscopy procedures in hybrid TIE2GFP-BALB/c transgenic mice, Mol. Imaging Biol. 223 (22) (2019) 486–493, https://doi.org/10.1007/S11307-019-01442-2.
[60] G. Kroemer, J. Pouyssegur, Tumor cell metabolism: cancer's Achilles' heel, Cancer Cell. 13 (2008) 472–482, https://doi.org/10.1016/J.CCR.2008.05.005.
[61] D. Hanahan, R.A. Weinberg, The hallmarks of cancer, Cell. 100 (2000) 57–70, https://doi.org/10.1016/S0092-8674(00)81683-9.
[62] M. Tong, I. McHardy, P. Ruegger, M. Goudarzi, P.C. Kashyap, T. Haritunians, X. Li, T.G. Graeber, E. Schwager, C. Huttenhower, A.J. Fornace, J.L. Sonnenburg, D. P. McGovern, J. Borneman, J. Braun, Reprograming of gut microbiome energy metabolism by the FUT2 Crohn's disease risk polymorphism, ISME J. 811 (8) (2014) 2193–2206, https://doi.org/10.1038/ismej.2014.64.
[63] D. Kapogiannis, M.P. Mattson, Disrupted energy metabolism and neuronal circuit dysfunction in cognitive impairment and Alzheimer's disease, Lancet Neurol. 10 (2011) 187–198, https://doi.org/10.1016/S1474-4422(10)70277-5.
[64] C.J. Fox, P.S. Hammerman, C.B. Thompson, Fuel feeds function: energy metabolism and the T-cell response, Nat. Rev. Immunol. 511 (5) (2005) 844–852, https://doi.org/10.1038/nri1710.
[65] C. Zhu, A.F. Martinez, H.L. Martin, M. Li, B.T. Crouch, D.A. Carlson, T.A.J. Haystead, N. Ramanujam, Near-simultaneous intravital microscopy of glucose uptake and mitochondrial membrane potential, key endpoints that reflect major metabolic axes in cancer, Sci. Rep. 7 (2017) 1–15, https://doi.org/10.1038/s41598-017-14226-x.
[66] M.C. Skala, K.M. Riching, D.K. Bird, A. Gendron-Fitzpatrick, J. Eickhoff, K.W. Eliceiri, P.J. Keely, N. Ramanujam, In vivo multiphoton fluorescence lifetime imaging of protein-bound and free nicotinamide adenine dinucleotide in normal and precancerous epithelia, J. Biomed. Opt. 12 (2007) 024014, https://doi.org/10.1117/1.2717503.
[67] M.G. Vander Heiden, L.C. Cantley, C.B. Thompson, Understanding the warburg effect: the metabolic requirements of cell proliferation NIH public access, Science (80-.). 324 (2009) 1029–1033. <https://doi.org/10.1126/science.1160809>.
[68] P.M. Schaefer, S. Kalinina, A. Rueck, C.A.F. von Arnim, B. von Einem, NADH autofluorescence—a marker on its way to boost bioenergetic research, Cytom. Part A 95 (2019) 34–46, https://doi.org/10.1002/CYTO.A.23597.
[69] T. Hato, S. Winfree, R. Day, R.M. Sandoval, B.A. Molitoris, M.C. Yoder, R.C. Wiggins, Y. Zheng, K.W. Dunn, P.C. Dagher, Two-photon intravital fluorescence lifetime imaging of the kidney reveals cell-type specific metabolic signatures, J. Am. Soc. Nephrol. 28 (2017) 2420–2430, https://doi.org/10.1681/ASN.2016101153.
[70] G.M. Thurber, K.S. Yang, T. Reiner, R.H. Kohler, P. Sorger, T. Mitchison, R. Weissleder, Single-cell and subcellular pharmacokinetic imaging allows insight into drug action in vivo, Nat. Commun. 4 (2013) 1504, https://doi.org/10.1038/NCOMMS2506.
[71] M.A. Miller, R. Weissleder, Imaging of anticancer drug action in single cells, Nat. Rev. Cancer 177 (17) (2017) 399–414, https://doi.org/10.1038/nrc.2017.41.
[72] A.M. Laughney, E. Kim, M.M. Sprachman, M.A. Miller, R.H. Kohler, K.S. Yang, J. D. Orth, T.J. Mitchison, R. Weissleder, Single-cell pharmacokinetic imaging reveals a therapeutic strategy to overcome drug resistance to the microtubule inhibitor eribulin, Sci. Transl. Med. 6 (2014), https://doi.org/10.1126/SCITRANSLMED.3009318/SUPPL_FILE/6-261RA152_SM.PDF.
[73] E.S. Nakasone, H.A. Askautrud, T. Kees, J.H. Park, V. Plaks, A.J. Ewald, M. Fein, M.G. Rasch, Y.X. Tan, J. Qiu, J. Park, P. Sinha, M.J. Bissell, E. Frengen, Z. Werb, M. Egeblad, Imaging tumor-stroma interactions during chemotherapy reveals contributions of the microenvironment to resistance, Cancer Cell. 21 (2012) 488–503, https://doi.org/10.1016/J.CCR.2012.02.017.
[74] R. Li, A. Attari, M. Prytyskach, M.A. Garlin, R. Weissleder, M.A. Miller, Single-cell intravital microscopy of trastuzumab quantifies heterogeneous in vivo kinetics, Cytom. Part A 97 (2020) 528–539, https://doi.org/10.1002/CYTO.A.23872.
[75] M.A. Miller, Y.-R. Zheng, S. Gadde, C. Pfirschke, H. Zope, C. Engblom, R.H. Kohler, Y. Iwamoto, K.S. Yang, B. Askevold, N. Kolishetti, M. Pittet, S.J. Lippard, O.C. Farokhzad, R. Weissleder, Tumour-associated macrophages act as a slow-release reservoir of nano-therapeutic Pt(IV) pro-drug, Nat. Commun. 61 (6) (2015) 1–13, https://doi.org/10.1038/ncomms9692.
[76] Z. Popović, W. Liu, V.P. Chauhan, J. Lee, C. Wong, A.B. Greytak, N. Insin, D.G. Nocera, D. Fukumura, R.K. Jain, M.G. Bawendi, A nanoparticle size series for in vivo fluorescence imaging, Angew. Chem. Int. Ed. 49 (2010) 8649–8652, https://doi.org/10.1002/anie.201003142.
[77] V.A. Naumenko, K.Y. Vlasova, A.S. Garanina, P.A. Melnikov, D.M. Potashnikova, D.A. Vishnevskiy, S.S. Vodopyanov, V.P. Chekhonin, M.A. Abakumov, A.G. Majouga, Extravasating neutrophils open vascular barrier and improve liposomes delivery to tumors, ACS Nano. 13 (2019) 12599–12612, https://doi.org/10.1021/acsnano.9b03848.
[78] A.M. Sofias, G. Bjørkøy, J. Ochando, L. Sønstevold, M. Hegvik, C. de L. Davies, O. Haraldseth, T. Lammers, W.J.M. Mulder, S. Hak, Cyclic arginine–glycine–aspartate-decorated lipid nanoparticle targeting toward inflammatory lesions involves hitchhiking with phagocytes, Adv. Sci. 8 (2021) 2100370. <https://doi.org/10.1002/ADVS.202100370>.
[79] S. Burkitt, M. Mehraein, R.K. Stanciauskas, J. Campbell, S. Fraser, C. Zavaleta, Label-free visualization and tracking of gold nanoparticles in vasculature using multiphoton luminescence, Nanomater 10 (2020) 2239. <https://doi.org/10.3390/NANO10112239>.
[80] B. Ouyang, W. Poon, Y. Zhang, Z. Lin, B. Kingston, A. Tavares, Y. Zhang, J. Chen, M. Valic, A. Syed, P. MacMillan, J. Couture-Senécal, G. Zheng, W. Chan, The dose threshold for nanoparticle tumour delivery, Nat. Mater. 19 (2020) 1362–1371, https://doi.org/10.1038/S41563-020-0755-Z.
[81] D. Pozebon, G.L. Scheffler, V.L. Dressler, Recent applications of laser ablation inductively coupled plasma mass spectrometry (LA-ICP-MS) for biological sample analysis: a follow-up review, J. Anal. At. Spectrom. 32 (2017) 890–919, https://doi.org/10.1039/C7JA00026J.
[82] J. Secklehner, C. Lo Celso, L.M. Carlin, Intravital microscopy in historic and contemporary immunology, Immunol. Cell Biol. 95 (2017) 506–513, https://doi.org/10.1038/ICB.2017.25.
[83] H.R. Manley, D.L. Potter, J.M. Heddleston, T.-L. Chew, M.C. Keightley, G.J. Lieschke, Frontline science: dynamic cellular and subcellular features of migrating leukocytes revealed by in vivo lattice lightsheet microscopy, J. Leukoc. Biol. 108 (2020) 455–468, https://doi.org/10.1002/JLB.3HI0120-589R.
[84] A. Marki, K. Buscher, Z. Mikulski, A. Pries, K. Ley, Rolling neutrophils form tethers and slings under physiologic conditions in vivo, J. Leukoc. Biol. 103 (2018) 67–70, https://doi.org/10.1189/JLB.1AB0617-230R.
[85] T. Lämmermann, P.V. Afonso, B.R. Angermann, J.M. Wang, W. Kastenmüller, C. A. Parent, R.N. Germain, Neutrophil swarms require LTB4 and integrins at sites of cell death in vivo, Nature. 498 (2013) 371–375, https://doi.org/10.1038/nature12175.
[86] F. Combes, A.M. Sofias, S. McCafferty, H. Huysmans, J. De Temmerman, S. Hak, E. Meyer, N.N. Sanders, Mononuclear but not polymorphonuclear phagocyte depletion increases circulation times and improves mammary tumor-homing efficiency of donor bone marrow-derived monocytes, Cancers 11 (2019) 1752. <https://doi.org/10.3390/CANCERS11111752>.
[87] B. McDonald, R. Davis, S. Kim, M. Tse, C. Esmon, E. Kolaczkowska, C. Jenne, Platelets and neutrophil extracellular traps collaborate to promote intravascular coagulation during sepsis in mice, Blood. 129 (2017) 1357–1367, https://doi.org/10.1182/BLOOD-2016-09-741298.
[88] V. Estrella, T. Chen, M. Lloyd, J. Wojtkowiak, H.H. Cornnell, A. Ibrahim-Hashim, K. Bailey, Y. Balagurunathan, J.M. Rothberg, B.F. Sloane, J. Johnson, R. A. Gatenby, R.J. Gillies, Acidity generated by the tumor microenvironment drives local invasion, Cancer Res. 73 (2013) 1524–1535, https://doi.org/10.1158/0008-5472.CAN-12-2796.
[89] B.J. Vakoc, R.M. Lanning, J.A. Tyrrell, T.P. Padera, L.A. Bartlett, T. Stylianopoulos, L.L. Munn, G.J. Tearney, D. Fukumura, R.K. Jain, B.E. Bouma, Three-dimensional microscopy of the tumor microenvironment in vivo using optical frequency domain imaging, Nat. Med. 1510 (15) (2009) 1219–1223, https://doi.org/10.1038/nm.1971.
[90] E.B. Brown, R.B. Campbell, Y. Tsuzuki, L. Xu, P. Carmeliet, D. Fukumura, R.K. Jain, M. EB, T. Y, X. L, C. RB, C. P, F. D, J. RK, In vivo measurement of gene expression, angiogenesis and physiological function in tumors using multiphoton laser scanning microscopy 7 (2001) 864–868. <https://doi.org/10.1038/89997>.
[91] C. Belli, D. Trapani, G. Viale, P. D'Amico, B.A. Duso, P. Della Vigna, F. Orsi, G. Curigliano, Targeting the microenvironment in solid tumors, Cancer Treat. Rev. 65 (2018) 22–32, https://doi.org/10.1016/J.CTRV.2018.02.004.
[92] M. Binnewies, E.W. Roberts, K. Kersten, V. Chan, D.F. Fearon, M. Merad, L.M. Coussens, D.I. Gabrilovich, S. Ostrand-Rosenberg, C.C. Hedrick, R.H. Vonderheide, M.J. Pittet, R.K. Jain, W. Zou, T.K. Howcroft, E.C. Woodhouse, R.A. Weinberg, M.F. Krummel, Understanding the tumor immune microenvironment (TIME) for effective therapy, Nat. Med. 245 (24) (2018) 541–550, https://doi.org/10.1038/s41591-018-0014-x.
[93] M.A. Miller, R. Weissleder, Imaging the pharmacology of nanomaterials by intravital microscopy: toward understanding their biological behavior, Adv. Drug Deliv. Rev. 113 (2017) 61–86, https://doi.org/10.1016/J.ADDR.2016.05.023.
[94] D.H. Madsen, H.J. Jürgensen, M.S. Siersbæk, D.E. Kuczek, L.G. Cloud, S. Liu, N. Behrendt, L. Grøntved, R. Weigert, T.H. Bugge, Tumor-associated macrophages derived from circulating inflammatory monocytes degrade collagen through cellular uptake, Cell Rep. 21 (2017) 3662–3671, https://doi.org/10.1016/J.CELREP.2017.12.011.
[95] Y. Chen, X. Liu, H. Yuan, Z. Yang, C.A. von Roemeling, Y. Qie, H. Zhao, Y. Wang, W. Jiang, B.Y.S. Kim, Therapeutic remodeling of the tumor microenvironment enhances nanoparticle delivery, Adv. Sci. 6 (2019) 1802070, https://doi.org/10.1002/ADVS.201802070.
[96] E. Hirata, M.R. Girotti, A. Viros, S. Hooper, B. Spencer-Dene, M. Matsuda, J. Larkin, R. Marais, E. Sahai, Intravital imaging reveals how BRAF inhibition generates drug-tolerant microenvironments with high integrin β1/FAK signaling, Cancer Cell. 27 (2015) 574–588, https://doi.org/10.1016/J.CCELL.2015.03.008.
[97] M. Turk, V. Naumenko, D.J. Mahoney, C.N. Jenne, Tracking cell recruitment and behavior within the tumor microenvironment using advanced intravital imaging approaches, Cells 7 (2018) 69. <https://doi.org/10.3390/CELLS7070069>.

[98] M.M. Janiurek, R. Soylu-Kucharz, C. Christoffersen, K. Kucharz, M. Lauritzen, Apolipoprotein M-bound sphingosine-1-phosphate regulates blood–brain barrier paracellular permeability and transcytosis, Elife 8 (2019), https://doi.org/10.7554/ELIFE.49405.
[99] O.A. Marcos-Contreras, C.F. Greineder, R.Y. Kiseleva, H. Parhiz, L.R. Walsh, V. Zuluaga-Ramirez, J.W. Myerson, E.D. Hood, C.H. Villa, I. Tombacz, N. Pardi, A. Seliga, B.L. Mui, Y.K. Tam, P.M. Glassman, V.V. Shuvaev, J. Nong, J.S. Brenner, M. Khoshnejad, T. Madden, D. Weissmann, Y. Persidsky, V.R. Muzykantov, Selective targeting of nanomedicine to inflamed cerebral vasculature to enhance the blood–brain barrier, Proc. Natl. Acad. Sci. U.S.A. 117 (2020) 3405–3414, https://doi.org/10.1073/PNAS.1912012117/SUPPL_FILE/PNAS.1912012117.SAPP.PDF.
[100] Z. Zhao, A. Ukidve, J. Kim, S. Mitragotri, Targeting strategies for tissue-specific drug delivery, Cell 181 (2020) 151–167, https://doi.org/10.1016/J.CELL.2020.02.001.
[101] S.K. Golombek, J.N. May, B. Theek, L. Appold, N. Drude, F. Kiessling, T. Lammers, Tumor targeting via EPR: strategies to enhance patient responses, Adv. Drug Deliv. Rev. 130 (2018) 17–38, https://doi.org/10.1016/J.ADDR.2018.07.007.
[102] H. Maeda, J. Wu, T. Sawa, Y. Matsumura, K. Hori, Tumor vascular permeability and the EPR effect in macromolecular therapeutics: a review, J. Control. Release. 65 (2000) 271–284, https://doi.org/10.1016/S0168-3659(99)00248-5.
[103] F. Danhier, To exploit the tumor microenvironment: since the EPR effect fails in the clinic, what is the future of nanomedicine?, J Control. Release. 244 (2016) 108–121, https://doi.org/10.1016/J.JCONREL.2016.11.015.
[104] Y. Matsumoto, J.W. Nichols, K. Toh, T. Nomoto, H. Cabral, Y. Miura, R.J. Christie, N. Yamada, T. Ogura, M.R. Kano, Y. Matsumura, N. Nishiyama, T. Yamasoba, Y.H. Bae, K. Kataoka, Vascular bursts enhance permeability of tumour blood vessels and improve nanoparticle delivery, Nat. Nanotechnol. 116 (11) (2016) 533–538, https://doi.org/10.1038/nnano.2015.342.
[105] M.A. Miller, R. Chandra, M.F. Cuccarese, C. Pfirschke, C. Engblom, S. Stapleton, U. Adhikary, R.H. Kohler, J.F. Mohan, M.J. Pittet, R. Weissleder, Radiation therapy primes tumors for nanotherapeutic delivery via macrophage-mediated vascular bursts, Sci. Transl. Med. 9 (2017), https://doi.org/10.1126/SCITRANSLMED.AAL0225/SUPPL_FILE/AAL0225_TABLE_S2.ZIP.
[106] J.I. Griffin, G. Wang, W.J. Smith, V.P. Vu, R. Scheinman, D. Stitch, R. Moldovan, S.M. Moghimi, D. Simberg, Revealing dynamics of accumulation of systemically injected liposomes in the skin by intravital microscopy, ACS Nano. 11 (2017) 11584–11593, https://doi.org/10.1021/ACSNANO.7B06524.
[107] S. Sindhwani, A.M. Syed, J. Ngai, B.R. Kingston, L. Maiorino, J. Rothschild, P. MacMillan, Y. Zhang, N.U. Rajesh, T. Hoang, J.L.Y. Wu, S. Wilhelm, A. Zilman, S. Gadde, A. Sulaiman, B. Ouyang, Z. Lin, L. Wang, M. Egeblad, W.C.W. Chan, The entry of nanoparticles into solid tumours, Nat. Mater. 195 (19) (2020) 566–575, https://doi.org/10.1038/s41563-019-0566-2.
[108] E. Phillips, O. Penate-Medina, P.B. Zanzonico, R.D. Carvajal, P. Mohan, Y. Ye, J. Humm, M. Gönen, H. Kalaigian, H. Schöder, H.W. Strauss, S.M. Larson, U. Wiesner, M.S. Bradbury, Clinical translation of an ultrasmall inorganic optical-PET imaging nanoparticle probe, Sci. Transl. Med. 6 (2014), https://doi.org/10.1126/SCITRANSLMED.3009524/SUPPL_FILE/6-260RA149_SM.PDF.
[109] M. Benezra, O. Penate-Medina, P.B. Zanzonico, D. Schaer, H. Ow, A. Burns, E. DeStanchina, V. Longo, E. Herz, S. Iyer, J. Wolchok, S.M. Larson, U. Wiesner, M. S. Bradbury, Multimodal silica nanoparticles are effective cancer-targeted probes in a model of human melanoma, J. Clin. Invest. 121 (2011) 2768, https://doi.org/10.1172/JCI45600.
[110] A.M. Sofias, Y.C. Toner, A.E. Meerwaldt, M.M.T. van Leent, G. Soultanidis, M. Elschot, H. Gonai, K. Grendstad, Å. Flobak, U. Neckmann, C. Wolowczyk, E.L. Fisher, T. Reiner, C. de L. Davies, G. Bjørkøy, A.J.P. Teunissen, J. Ochando, C. Pérez-Medina, W.J.M. Mulder, S. Hak, Tumor targeting by αvβ3-integrin-specific lipid nanoparticles occurs via phagocyte hitchhiking, ACS Nano. 14 (2020) 7832–7846. <https://doi.org/10.1021/ACSNANO.9B08693>.
[111] B.R. Smith, E.E.B. Ghosn, H. Rallapalli, J.A. Prescher, T. Larson, L.A. Herzenberg, S.S. Gambhir, Selective uptake of single-walled carbon nanotubes by circulating monocytes for enhanced tumour delivery, Nat. Nanotechnol. 9 (2014) 481–487, https://doi.org/10.1038/nnano.2014.62.
[112] D. Chu, J. Gao, Z. Wang, Neutrophil-mediated delivery of therapeutic nanoparticles across blood vessel barrier for treatment of inflammation and infection, ACS Nano. 9 (2015) 11800–11811, https://doi.org/10.1021/ACSNANO.5B05583/SUPPL_FILE/NN5B05583_SI_003.AVI.
[113] V.A. Naumenko, S.S. Vodopyanov, K.Y. Vlasova, D.M. Potashnikova, P.A. Melnikov, D.A. Vishnevskiy, A.S. Garanina, M.P. Valikhov, A.V. Lipatova, V.P. Chekhonin, A.G. Majouga, M.A. Abakumov, Intravital imaging of liposome behavior upon repeated administration: a step towards the development of liposomal companion diagnostic for cancer nanotherapy, J. Control. Release. 330 (2021) 244–256, https://doi.org/10.1016/J.JCONREL.2020.12.014.
[114] S.P. Arlauckas, C.S. Garris, R.H. Kohler, M. Kitaoka, M.F. Cuccarese, K.S. Yang, M.A. Miller, J.C. Carlson, G.J. Freeman, R.M. Anthony, R. Weissleder, M.J. Pittet, In vivo imaging reveals a tumor-associated macrophage-mediated resistance pathway in anti-PD-1 therapy, Sci. Transl. Med. 9 (2017), https://doi.org/10.1126/SCITRANSLMED.AAL3604/SUPPL_FILE/AAL3604_SM.PDF.
[115] G. Germano, R. Frapolli, C. Belgiovine, A. Anselmo, S. Pesce, M. Liguori, E. Erba, S. Uboldi, M. Zucchetti, F. Pasqualini, M. Nebuloni, N. van Rooijen, R. Mortarini, L. Beltrame, S. Marchini, I. Fuso Nerini, R. Sanfilippo, P.G. Casali, S. Pilotti, C.M. Galmarini, A. Anichini, A. Mantovani, M. D'Incalci, P. Allavena, Role of macrophage targeting in the antitumor activity of trabectedin, Cancer Cell. 23 (2013) 249–262, https://doi.org/10.1016/J.CCR.2013.01.008.
[116] B. Priem, M.M.T. van Leent, A.J.P. Teunissen, A.M. Sofias, V.P. Mourits, L. Willemsen, E.D. Klein, R.S. Oosterwijk, A.E. Meerwaldt, J. Munitz, G. Prévot, A. Vera Verschuur, S.A. Nauta, E.M. van Leeuwen, E.L. Fisher, K.A.M. de Jong, Y. Zhao, Y.C. Toner, G. Soultanidis, C. Calcagno, P.H.H. Bomans, H. Friedrich, N. Sommerdijk, T. Reiner, R. Duivenvoorden, E. Zupančič, J.S. Di Martino, E. Kluza, M. Rashidian, H.L. Ploegh, R.M. Dijkhuizen, S. Hak, C. Pérez-Medina, J.J. Bravo-Cordero, M.P.J. de Winther, L.A.B. Joosten, A. van Elsas, Z.A. Fayad, A. Rialdi, D. Torre, E. Guccione, J. Ochando, M.G. Netea, A.W. Griffioen, W.J.M. Mulder, Trained immunity-promoting nanobiologic therapy suppresses tumor growth and potentiates checkpoint inhibition, Cell 183 (2020) 786–801.e19, https://doi.org/10.1016/J.CELL.2020.09.059.
[117] T. Luedde, N. Kaplowitz, R.F. Schwabe, Cell death and cell death responses in liver disease: mechanisms and clinical relevance, Gastroenterology 147 (2014) 765–783.e4, https://doi.org/10.1053/J.GASTRO.2014.07.018.
[118] B.R. Stockwell, J.P. Friedmann Angeli, H. Bayir, A.I. Bush, M. Conrad, S.J. Dixon, S. Fulda, S. Gascón, S.K. Hatzios, V.E. Kagan, K. Noel, X. Jiang, A. Linkermann, M.E. Murphy, M. Overholtzer, A. Oyagi, G.C. Pagnussat, J. Park, Q. Ran, C.S. Rosenfeld, K. Salnikow, D. Tang, F.M. Torti, S. V. Torti, S. Toyokuni, K.A. Woerpel, D.D. Zhang, Ferroptosis: a regulated cell death nexus linking metabolism, redox biology, and Disease, Cell 171 (2017) 273–285. <https://doi.org/10.1016/J.CELL.2017.09.021>.
[119] G. Kroemer, L. Galluzzi, O. Kepp, L. Zitvogel, Immunogenic cell death in cancer therapy, Http://Dx.Doi.Org/10.1146/Annurev-Immunol-032712-100008 31 (2013) 51–72, https://doi.org/10.1146/ANNUREV-IMMUNOL-032712-100008.
[120] D.R. Green, J.C. Reed, Mitochondria and apoptosis, New Ser. 281 (1998) 1309–1312.
[121] L. Galluzzi, I. Vitale, S.A. Aaronson, J.M. Abrams, D. Adam, P. Agostinis, E.S. Alnemri, L. Altucci, I. Amelio, D.W. Andrews, M. Annicchiarico-Petruzzelli, A. V. Antonov, E. Arama, E.H. Baehrecke, N.A. Barlev, N.G. Bazan, F. Bernassola, M.J.M. Bertrand, K. Bianchi, M.V. Blagosklonny, K. Blomgren, C. Borner, P. Boya, C. Brenner, M. Campanella, E. Candi, D. Carmona-Gutierrez, F. Cecconi, F.K.M. Chan, N.S. Chandel, E.H. Cheng, J.E. Chipuk, J.A. Cidlowski, A. Ciechanover, G.M. Cohen, M. Conrad, J.R. Cubillos-Ruiz, P.E. Czabotar, V. D'Angiolella, T.M. Dawson, V.L. Dawson, V. De Laurenzi, R. De Maria, K.M. Debatin, R.J. Deberardinis, M. Deshmukh, N. Di Daniele, F. Di Virgilio, V.M. Dixit, S.J. Dixon, C.S. Duckett, B.D. Dynlacht, W.S. El-Deiry, J.W. Elrod, G.M. Fimia, S. Fulda, A.J. García-Sáez, A.D. Garg, C. Garrido, E. Gavathiotis, P. Golstein, E. Gottlieb, D.R. Green, L.A. Greene, H. Gronemeyer, A. Gross, G. Hajnoczky, J.M. Hardwick, I.S. Harris, M.O. Hengartner, C. Hetz, H. Ichijo, M. Jäättelä, B. Joseph, P.J. Jost, P.P. Juin, W.J. Kaiser, M. Karin, T. Kaufmann, O. Kepp, A. Kimchi, R.N. Kitsis, D.J. Klionsky, R.A. Knight, S. Kumar, S.W. Lee, J.J. Lemasters, B. Levine, A. Linkermann, S.A. Lipton, R.A. Lockshin, C. López-Otín, S.W. Lowe, T. Luedde, E. Lugli, M. MacFarlane, F. Madeo, M. Malewicz, W. Malorni, G. Manic, J.C. Marine, S.J. Martin, J.C. Martinou, J.P. Medema, P. Mehlen, P. Meier, S. Melino, E.A. Miao, J.D. Molkentin, U.M. Moll, C. Muñoz-Pinedo, S. Nagata, G. Nuñez, A. Oberst, M. Oren, M. Overholtzer, M. Pagano, T. Panaretakis, M. Pasparakis, J.M. Penninger, D.M. Pereira, S. Pervaiz, M.E. Peter, M. Piacentini, P. Pinton, J.H.M. Prehn, H. Puthalakath, G.A. Rabinovich, M. Rehm, R. Rizzuto, C.M.P. Rodrigues, D.C. Rubinsztein, T. Rudel, K.M. Ryan, E. Sayan, L. Scorrano, F. Shao, Y. Shi, J. Silke, H.U. Simon, A. Sistigu, B.R. Stockwell, A. Strasser, G. Szabadkai, S.W.G. Tait, D. Tang, N. Tavernarakis, A. Thorburn, Y. Tsujimoto, B. Turk, T. Vanden Berghe, P. Vandenabeele, M.G. Vander Heiden, A. Villunger, H.W. Virgin, K.H. Vousden, D. Vucic, E.F. Wagner, H. Walczak, D. Wallach, Y. Wang, J.A. Wells, W. Wood, J. Yuan, Z. Zakeri, B. Zhivotovsky, L. Zitvogel, G. Melino, G. Kroemer, Molecular mechanisms of cell death: recommendations of the nomenclature committee on cell death 2018, Cell Death Differ. 25 (2018) 486–541, https://doi.org/10.1038/s41418-017-0012-4.
[122] I.M. Schießl, A. Hammer, A. Riquier-Brison, J. Peti-Peterdi, Just look! intravital microscopy as the best means to study kidney cell death dynamics, Semin. Nephrol. 36 (2016) 220–236, https://doi.org/10.1016/J.SEMNEPHROL.2016.03.009.
[123] P. Yang, J.R. Smith, K.S. Damodar, S.R. Planck, J.T. Rosenbaum, Visualization of cell death in vivo during murine endotoxin-induced uveitis, Invest. Ophthalmol. Vis. Sci. 44 (2003) 1993–1997, https://doi.org/10.1167/IOVS.02-0582.
[124] A. Janssen, E. Beerling, R. Medema, J. van Rheenen, Intravital FRET imaging of tumor cell viability and mitosis during chemotherapy, PLoS One. 8 (2013) e64029.
[125] I.M. Schießl, A. Hammer, V. Kattler, B. Gess, F. Theilig, R. Witzgall, H. Castrop, Intravital imaging reveals angiotensin ii–induced transcytosis of albumin by podocytes, J. Am. Soc. Nephrol. 27 (2016) 731–744, https://doi.org/10.1681/ASN.2014111125.
[126] Z.G. Fridlender, J. Sun, S. Kim, V. Kapoor, G. Cheng, L. Ling, G.S. Worthen, S.M. Albelda, Polarization of Tumor-Associated Neutrophil (TAN) phenotype by TGF-β: "N1" versus "N2" TAN, Cancer Cell. 16 (2009) 183, https://doi.org/10.1016/J.CCR.2009.06.017.
[127] C. Silvestre-Roig, Z.G. Fridlender, M. Glogauer, P. Scapini, Neutrophil diversity in health and disease, Trends Immunol. 40 (2019) 565, https://doi.org/10.1016/J.IT.2019.04.012.
[128] L.G. Ng, R. Ostuni, A. Hidalgo, Heterogeneity of neutrophils, Nat. Rev. Immunol. 194 (19) (2019) 255–265, https://doi.org/10.1038/s41577-019-0141-8.
[129] E. Kolaczkowska, C.N. Jenne, B.G.J. Surewaard, A. Thanabalasuriar, W.Y. Lee, M.J. Sanz, K. Mowen, G. Opdenakker, P. Kubes, Molecular mechanisms of NET

formation and degradation revealed by intravital imaging in the liver vasculature, Nat. Commun. 61 (6) (2015) 1–13, https://doi.org/10.1038/ncomms7673.
[130] S.B. Cohen, B.H. Gern, J.L. Delahaye, K.N. Adams, C.R. Plumlee, J.K. Winkler, D. R. Sherman, M.Y. Gerner, K.B. Urdahl, Alveolar macrophages provide an early mycobacterium tuberculosis niche and initiate dissemination, Cell Host Microbe. 24 (2018) 439–446.e4, https://doi.org/10.1016/J.CHOM.2018.08.001.
[131] A.M. Mowat, C.L. Scott, C.C. Bain, Barrier-tissue macrophages: functional adaptation to environmental challenges, Nat. Med. 2311 (23) (2017) 1258–1270, https://doi.org/10.1038/nm.4430.
[132] K. Westphalen, G.A. Gusarova, M.N. Islam, M. Subramanian, T.S. Cohen, A.S. Prince, J. Bhattacharya, Sessile alveolar macrophages communicate with alveolar epithelium to modulate immunity, Nature 5067489 (506) (2014) 503–506, https://doi.org/10.1038/nature12902.
[133] K. Westphalen, G.A. Gusarova, M.N. Islam, M. Subramanian, T.S. Cohen, A.S. Prince, J. Bhattacharya, Sessile alveolar macrophages modulate immunity through connexin 43-based epithelial communication, Nature 506 (2014) 503, https://doi.org/10.1038/NATURE12902.
[134] J. Bhattacharya, K. Westphalen, Macrophage-epithelial interactions in pulmonary alveoli, Semin. Immunopathol. 384 (38) (2016) 461–469, https://doi.org/10.1007/S00281-016-0569-X.
[135] A.S. Neupane, M. Willson, A.K. Chojnacki, F. Vargas E Silva Castanheira, C. Morehouse, A. Carestia, A.E. Keller, M. Peiseler, A. DiGiandomenico, M.M. Kelly, M. Amrein, C. Jenne, A. Thanabalasuriar, P. Kubes, Patrolling Alveolar Macrophages Conceal Bacteria from the Immune System to Maintain Homeostasis, Cell. 183 (2020) 110–125.e11. <https://doi.org/10.1016/J.CELL.2020.08.020>.
[136] M. De Niz, A. Nacer, F. Frischknecht, Intravital microscopy: Imaging host–parasite interactions in the brain, Cell. Microbiol. 21 (2019) e13024.
[137] J. van Rheenen, C.L.G.J. Scheele, Intravital microscopy to illuminate cell state plasticity during metastasis, Curr. Opin. Cell Biol. 72 (2021) 28–35, https://doi.org/10.1016/J.CEB.2021.04.004.
[138] C.D. Paul, P. Mistriotis, K. Konstantopoulos, Cancer cell motility: lessons from migration in confined spaces, Nat. Rev. Cancer 2016 172. 17 (2016) 131–140. <https://doi.org/10.1038/nrc.2016.123>.
[139] M. De Palma, M.A. Venneri, R. Galli, L.S. Sergi, L.S. Politi, M. Sampaolesi, L. Naldini, Tie2 identifies a hematopoietic lineage of proangiogenic monocytes required for tumor vessel formation and a mesenchymal population of pericyte progenitors, Cancer Cell. 8 (2005) 211–226, https://doi.org/10.1016/J.CCR.2005.08.002.
[140] E.Y. Lin, J.-F. Li, L. Gnatovskiy, Y. Deng, L. Zhu, D.A. Grzesik, H. Qian, X. Xue, J. W. Pollard, Macrophages regulate the angiogenic switch in a mouse model of breast cancer, Cancer Res. 66 (2006) 11238–11246, https://doi.org/10.1158/0008-5472.CAN-06-1278.
[141] B.D. Robinson, G.L. Sica, Y.-F. Liu, T.E. Rohan, F.B. Gertler, J.S. Condeelis, J.G. Jones, Tumor microenvironment of metastasis in human breast carcinoma: a potential prognostic marker linked to hematogenous dissemination, Clin. Cancer Res. 15 (2009) 2433, https://doi.org/10.1158/1078-0432.CCR-08-2179.
[142] M. Roh-Johnson, J.J. Bravo-Cordero, A. Patsialou, V.P. Sharma, P. Guo, H. Liu, L. Hodgson, J. Condeelis, Macrophage contact induces RhoA GTPase signaling to trigger tumor cell intravasation, Oncogene. 33 (2014) 4203, https://doi.org/10.1038/ONC.2013.377.
[143] A.S. Harney, E.N. Arwert, D. Entenberg, Y. Wang, P. Guo, B.-Z. Qian, M.H. Oktay, J.W. Pollard, J.G. Jones, J.S. Condeelis, Real-time imaging reveals local, transient vascular permeability and tumor cell intravasation stimulated by Tie2Hi macrophage-derived VEGFA, Cancer Discov. 5 (2015) 932, https://doi.org/10.1158/2159-8290.CD-15-0012.
[144] E. D'Asti, D. Garnier, T.H. Lee, L. Montermini, B. Meehan, J. Rak, Oncogenic extracellular vesicles in brain tumor progression, Front. Physiol. 3 (2012), https://doi.org/10.3389/FPHYS.2012.00294.
[145] K.C. Vickers, B.T. Palmisano, B.M. Shoucri, R.D. Shamburek, A.T. Remaley, MicroRNAs are transported in plasma and delivered to recipient cells by high-density lipoproteins, Nat. Cell Biol. 134 (13) (2011) 423–433, https://doi.org/10.1038/ncb2210.
[146] J. Skog, T. Würdinger, S. van Rijn, D.H. Meijer, L. Gainche, W.T. Curry, B.S. Carter, A.M. Krichevsky, X.O. Breakefield, Glioblastoma microvesicles transport RNA and proteins that promote tumour growth and provide diagnostic biomarkers, Nat. Cell Biol. 1012 (10) (2008) 1470–1476, https://doi.org/10.1038/ncb1800.
[147] van der V. KE, A. ER, Z. X, L. C, C. E, O. D, P. S, M. O, C. MH, S. J, K. AM, S.-R. A, M. TR, E.K. J, H. SE, B. XO, Directly visualized glioblastoma-derived extracellular vesicles transfer RNA to microglia/macrophages in the brain, Neuro. Oncol. 18 (2016) 58–69. <https://doi.org/10.1093/NEUONC/NOV244>.
[148] Y. Fuchs, H. Steller, Programmed cell death in animal development and disease, Cell 147 (2011) 742–758, https://doi.org/10.1016/J.CELL.2011.10.033.
[149] M. Sarhan, A. von Mässenhausen, C. Hugo, R. Oberbauer, A. Linkermann, Immunological consequences of kidney cell death, Cell Death Dis. 92 (9) (2018) 1–15, https://doi.org/10.1038/s41419-017-0057-9.
[150] D.L. Rosin, M.D. Okusa, Dangers within: DAMP responses to damage and cell death in kidney disease, J. Am. Soc. Nephrol. 22 (2011) 416–425, https://doi.org/10.1681/ASN.2010040430.
[151] L. A, C. G, D. G, K. U, K. S, D. Z, Regulated cell death in AKI, J. Am. Soc. Nephrol. 25 (2014) 2689–2701. <https://doi.org/10.1681/ASN.2014030262>.
[152] J. Peti-Peterdi, S. Morishima, T. Miyoshi, P.D. Bell, Y. Okada, Macula densa cell water transport assessed by two-photon laser scanning fluorescence microscopy, FASEB J. 14 (2000).
[153] P. Cl, A. Lj, F. Aj, K. Dj, C. Jl, F. s, d. kw,, Three-dimensional imaging of embryonic mouse kidney by two-photon microscopy, Am. J. Pathol. 158 (2001) 49–55, https://doi.org/10.1016/S0002-9440(10)63943-0.
[154] T. Hato, S. Winfree, P.C. Dagher, Kidney imaging: – intravital microscopy, Methods Mol. Biol. 1763 (2018) 129, https://doi.org/10.1007/978-1-4939-7762-8_12.
[155] N. Baudry, E. Laemmel, E. Vicaut, In vivo reactive oxygen species production induced by ischemia in muscle arterioles of mice: involvement of xanthine oxidase and mitochondria, Https://Doi.Org/10.1152/Ajpheart.00378.2007 294 (2008) 821–828, https://doi.org/10.1152/AJPHEART.00378.2007.
[156] H. Am, R. Gj, S. Rm, C. Pr, M. Ba, In vivo multiphoton imaging of mitochondrial structure and function during acute kidney injury, Kidney Int. 83 (2013) 72–83, https://doi.org/10.1038/KI.2012.328.
[157] J.S. Di Martino, A.R. Nobre, C. Mondal, I. Taha, E.F. Farias, E.J. Fertig, A. Naba, J. A. Aguirre-Ghiso, J.J. Bravo-Cordero, A tumor-derived type III collagen-rich ECM niche regulates tumor cell dormancy, Nat. Cancer 2021 31. 3 (2021) 90–107. <https://doi.org/10.1038/s43018-021-00291-9>.
[158] J.M. Niers, J.W. Chen, G. Lewandrowski, M. Kerami, E. Garanger, G. Wojtkiewicz, P. Waterman, E. Keliher, R. Weissleder, B.A. Tannous, Single reporter for targeted multimodal in vivo imaging, J. Am. Chem. Soc. 134 (2012) 5149–5156, https://doi.org/10.1021/JA209868G/SUPPL_FILE/JA209868G_SI_001.PDF.
[159] M. Giampetraglia, B. Weigelin, Recent advances in intravital microscopy for preclinical research, Curr. Opin. Chem. Biol. 63 (2021) 200–208, https://doi.org/10.1016/J.CBPA.2021.05.010.
[160] J. Ko, K. Lucas, R. Kohler, E.A. Halabi, M. Wilkovitsch, J.C.T. Carlson, R. Weissleder, In vivo click chemistry enables multiplexed intravital microscopy, Adv. Sci. (2022) 2200064, https://doi.org/10.1002/ADVS.202200064.
[161] K. Zhang, S. Chen, H. Sun, L. Wang, H. Li, J. Zhao, C. Zhang, N. Li, Z. Guo, Z. Han, Z.C. Han, G. Zheng, X. Chen, Z. Li, In vivo two-photon microscopy reveals the contribution of Sox9+ cell to kidney regeneration in a mouse model with extracellular vesicle treatment, J. Biol. Chem. 295 (2020) 12203–12213, https://doi.org/10.1074/JBC.RA120.012732/ATTACHMENT/15EE30CD-5EDD-4B06-B990-ACB74F7E5A06/MMC1.ZIP.
[162] H.E. Brighton, S.P. Angus, T. Bo, J. Roques, A.C. Tagliatela, D.B. Darr, K. Karagoz, N. Sciaky, M.L. Gatza, N.E. Sharpless, G.L. Johnson, J.E. Bear, New mechanisms of resistance to MEK inhibitors in melanoma revealed by intravital imaging, Cancer Res. 78 (2018) 542–557, https://doi.org/10.1158/0008-5472.CAN-17-1653/657811/AM/NEW-MECHANISMS-OF-RESISTANCE-TO-MEK-INHIBITORS-IN.
[163] T. Masuda, L. Amann, R. Sankowski, O. Staszewski, M. Lenz, P. dErrico, N. Snaidero, M.J. Costa Jordão, C. Böttcher, K. Kierdorf, S. Jung, J. Priller, T. Misgeld, A. Vlachos, M.M. Luehmann, K.P. Knobeloch, M. Prinz, Novel Hexb-based tools for studying microglia in the CNS, Nat. Immunol. 2020 217. 21 (2020) 802–815. <https://doi.org/10.1038/s41590-020-0707-4>.
[164] E.M. Gabriel, D.T. Fisher, S. Evans, K. Takabe, J.J. Skitzki, Intravital microscopy in the study of the tumor microenvironment: from bench to human application, Oncotarget. 9 (2018) 20165, https://doi.org/10.18632/ONCOTARGET.24957.
[165] B.-G. Wang, K. König, K.-J. Halbhuber, Two-photon microscopy of deep intravital tissues and its merits in clinical research, J. Microsc. 238 (2010) 1–20, https://doi.org/10.1111/J.1365-2818.2009.03330.X.
[166] E.M. Gabriel, M. Kim, D.T. Fisher, C. Mangum, K. Attwood, W. Ji, D. Mukhopadhyay, S.P. Bagaria, M.W. Robertson, T.A. Dinh, K.L. Knutson, J.J. Skitzki, M.B. Wallace, A pilot trial of intravital microscopy in the study of the tumor vasculature of patients with peritoneal carcinomatosis, Sci. Reports 111 (11) (2021) 1–13, https://doi.org/10.1038/s41598-021-84430-3.
[167] Mayo Clinic, Intravital Microscopy (IVM) in Patients With Peritoneal Carcinomatosis (PC) - Full Text View - ClinicalTrials.gov, (n.d.). <https://clinicaltrials.gov/ct2/show/NCT03517852?term=NCT03517852&draw=2> (Accessed September 3, 2021).
[168] Mayo Clinic, A Study of Intravital Microscopy (IVM) in Human Solid Tumors - Mayo Clinic, (n.d.). <https://www.mayo.edu/research/clinical-trials/cls-20453746> (Accessed September 3, 2021).
[169] W. Becker, L. Braun, Metabolic FLIM at the dawn of clinical application, 11648 (2021) 116480J. <https://doi.org/10.1117/12.2578319>.
[170] A. Rück, P. Schäfer, B. von Einem, I.S. Kritchenkov, S. Kalinina, Metabolic NADH/FAD/FMN FLIM and oxygen PLIM: multiphoton luminescence lifetime imaging on the way to clinical diagnosis 11244 (2020) 112440M. <https://doi.org/10.1117/12.2546095>.
[171] Z. Wang, Y. Zheng, D. Zhao, Z. Zhao, L. Liu, A. Pliss, F. Zhu, J. Liu, J. Qu, P. Luan, Applications of fluorescence lifetime imaging in clinical medicine, https://Doi.Org/10.1142/S179354581830001X. 11 (2017). https://doi.org/10.1142/S179354581830001X.
[172] Y. Ouyang, Y. Liu, Z.M. Wang, Z. Liu, M. Wu, FLIM as a promising tool for cancer diagnosis and treatment monitoring, Nano-Micro Lett. 131 (13) (2021) 1–27, https://doi.org/10.1007/S40820-021-00653-Z.
[173] H. Studier, Y.S. Mohammed, M.S. Roberts, A. Holmes, M. Pastore, W. Becker, Multiphoton FLIM is gaining ground as a clinical tool (Conference Presentation), SPIE (2020) 112441Q, https://doi.org/10.1117/12.2544795.
[174] T. Ching, D.S. Himmelstein, B.K. Beaulieu-Jones, A.A. Kalinin, B.T. Do, G.P. Way, E. Ferrero, P.M. Agapow, M. Zietz, M.M. Hoffman, W. Xie, G.L. Rosen, B.J.

Lengerich, J. Israeli, J. Lanchantin, S. Woloszynek, A.E. Carpenter, A. Shrikumar, J. Xu, E.M. Cofer, C.A. Lavender, S.C. Turaga, A.M. Alexandari, Z. Lu, D.J. Harris, D. Decaprio, Y. Qi, A. Kundaje, Y. Peng, L.K. Wiley, M.H.S. Segler, S.M. Boca, S.J. Swamidass, A. Huang, A. Gitter, C.S. Greene, Opportunities and obstacles for deep learning in biology and medicine, J. R. Soc. Interface. 15 (2018), https://doi.org/10.1098/RSIF.2017.0387.

[175] D.R. Chittajallu, S. Florian, R.H. Kohler, Y. Iwamoto, J.D. Orth, R. Weissleder, G. Danuser, T.J. Mitchison, In vivo cell-cycle profiling in xenograft tumors by quantitative intravital microscopy, Nat. Methods 126 (12) (2015) 577–585, https://doi.org/10.1038/nmeth.3363.

[176] B.C. Gregório da Silva, R. Tam, R.J. Ferrari, Detecting cells in intravital video microscopy using a deep convolutional neural network, Comput. Biol. Med. 129 (2021) 104133, https://doi.org/10.1016/J.COMPBIOMED.2020.104133.

[177] S.E. Coffey, R.J. Giedt, R. Weissleder, Automated analysis of clonal cancer cells by intravital imaging, IntraVital. 2 (2013) 1–9, https://doi.org/10.4161/INTV.26138/SUPPL_FILE/KINV_A_10926138_SM0001.ZIP.

[178] B. Gligorijevic, A. Bergman, J. Condeelis, Multiparametric classification links tumor microenvironments with tumor cell phenotype, PLoS Biol. 12 (2014) 1001995, https://doi.org/10.1371/JOURNAL.PBIO.1001995.

[179] T. Falk, D. Mai, R. Bensch, Ö. Çiçek, A. Abdulkadir, Y. Marrakchi, A. Böhm, J. Deubner, Z. Jäckel, K. Seiwald, A. Dovzhenko, O. Tietz, C. Dal Bosco, S. Walsh, D. Saltukoglu, T.L. Tay, M. Prinz, K. Palme, M. Simons, I. Diester, T. Brox, O. Ronneberger, U-Net: deep learning for cell counting, detection, and morphometry, Nat. Methods 161 (16) (2018) 67–70, https://doi.org/10.1038/s41592-018-0261-2.

[180] E. Moen, D. Bannon, T. Kudo, W. Graf, M. Covert, D. Van Valen, Deep learning for cellular image analysis, Nat. Methods 1612 (16) (2019) 1233–1246, https://doi.org/10.1038/s41592-019-0403-1.

[181] D.M. Camacho, K.M. Collins, R.K. Powers, J.C. Costello, J.J. Collins, Next-generation machine learning for biological networks, Cell 173 (2018) 1581–1592, https://doi.org/10.1016/J.CELL.2018.05.015.

[182] J.L. Hor, R.N. Germain, Intravital and high-content multiplex imaging of the immune system, Trends Cell Biol. (2021), https://doi.org/10.1016/J.TCB.2021.11.007.